.NASA TM-86414

NASA Technical Memorandum 86414

STUDY OF AN EFFICIENT LONG-RANGE MACH 2.7 SUPERSONIC TRANSPORT CONFIGURATION CONCEPT

PETER D. GALL

JULY 1985

National Aeronautics and
Space Administration

Langley Research Center
Hampton, Virginia 23665

INTRODUCTION

Commercial supersonic transports offer the possibility of large reductions in travel time as well as major increases in productivity. Unfortunately, the only current supersonic transport is too marginal in range, payload, and fuel consumption to be completely viable in this category.

The past twenty years have seen major improvements in many of the technologies applicable to supersonic transports (ref. 1). Several prior studies (refs. 2-5) have applied some of these improvements to supersonic design concepts for a 270-290 passenger, Mach 2.7, arrow-wing type transport configuration. The design mission range was typically 3800-4500 nautical miles, and maximum takeoff gross weights varied from 640,000 to 750,000 pounds. Utilizing the most updated analytical methods (refs. 6-13) for calculating skin-friction drag, roughness drag, wave drag, and drag due to lift, the operating maximum lift-drag ratio for these configurations was computed to be about nine.

It is the purpose of this study to develop, using similar analytical methods, an aerodynamically improved, arrow-wing canard configuration. The aircraft is intended to be consistent with the AST-205 configuration with regard to passenger-carrying capability and passenger comfort. The AST-205 is one of the most recent advanced supersonic transport configurations to come out of previous studies (ref. 5).

Several wing-body-canard lifting systems were carefully studied and gradually refined. In addition, complete configuration mass, balance, and trim characteristics were evaluated in close coordination with the lifting system's lift, drag, and pitching moment characteristics. Once the aerodynamics and mass properties were determined, these values were used in a sizing and performance computer program (ref. 14) to refine the mass properties and fuel requirements, as well as to determine optimum thrust loading and wing loading. The design range was chosen to be 6,000 nautical miles based on the discussion of reference 15. An aircraft of this range capability would permit nonstop travel from New York to any point in Europe, South America, China, Japan, India, northern and western parts of Africa, and Central Asia. Also, it would permit direct flights from Los Angeles to Australia, South America, the USSR, and all of Northern Europe. At the same time, flights of 6 hours, including 1-hour stopovers for refueling, could cover a 9,000-mile range.

The results obtained from the sizing and performance evaluation were then used to refine a final configuration designated as the CST-11. A final performance evaluation was completed to insure that the aircraft met the design goals.

SYMBOLS

b	overall span, ft
c	chord
C_D	total drag coefficient

C_{D_i}	induced drag coefficient
C_{D_F}	friction drag coefficient
C_{D_R}	roughness drag coefficient
C_{D_W}	wave drag coefficient
C_M	pitching moment coefficient
C_{M_0}	zero-lift pitching moment coefficient
C_p	pressure coefficient
$C_{p_{vac}}$	vacuum pressure coefficient
c.g.	center of gravity
$\frac{\partial C_D}{\partial C_L^2}$	induced drag-due-to-lift factor
C_L	lift coefficient
D	drag force, lbf
i_c	canard incidence angle (positive trailing edge down) deg
L/D	lift-drag ratio
L/D_{MAX}	maximum lift-drag ratio
M	Mach number
MAC	mean aerodynamic chord, ft
P_{t_1}/P_{t_2}	inlet pressure recovery
q	dynamic pressure, lbf/ft^2
S	wing reference area, ft^2
$t/_c$	thickness ratio
$T/_W$	thrust-weight ratio
$W/_S$	wing loading, $\frac{lbf}{ft^2}$
X	longitudinal coordinate, ft

Y	lateral coordinate, ft
Z	vertical coordinate, ft
δ_{T_1}	outboard flaperon deflection (positive down), deg
δ_{T_2}	inboard flap deflection (positive down), deg
Λ_{LE}	leading-edge sweep, deg

CONFIGURATION DEVELOPMENT

The configuration developed in this study originated as a highly-swept supersonic tailless arrow wing. From a strictly aerodynamic point of view, the tailless configuration appears attractive. The wetted area to wing-area ratio approaches 2.0, which is optimum for minimum viscous skin-friction drag. The area distribution curve of a highly-swept wing is smooth and bell shaped, resulting in low wave drag. Finally, the arrow wing is efficient in terms of induced drag, although it does exhibit inherently poor pitch-up characteristics at high angles of attack due to flow separation at the thin outboard cranked tip. After a brief analysis conducted in this study, it was determined that the tailless arrow-wing configuration may possess some stability and control problems. To maintain positive static stability and positive zero-lift pitching moment, the wing trailing edge must be reflexed. Reflexing can penalize the induced drag efficiency. Controllability of an all-flying wing may also be a problem since the configuration must be controllable throughout the c.g. range, as well as the a.c. range which shifts with Mach number. Based on these considerations, the present configuration study evolved from a modified tailless arrow-wing configuration to a canard-arrow-wing configuration.

A long forebody was added to the basic highly-swept arrow-wing planform. The forebody, or fuselage, was elliptical in cross section and was blended into the basic wing. The fuselage was sized to hold approximately 275-300 passengers plus crew. The wing was originally estimated to have approximately 10,000 square feet of wing area. For balance, the four engines were placed in a common cluster located as far rearward as possible.

A brief mass and balance analysis showed that some type of forward control surface would be required for good trim and control characteristics. The analysis also showed that with a large forward surface (canard area approximately 10% of the wing area) and a rearward c.g. location, positive static stability would exist. In addition, the canard must carry some positive load during cruise flight, even at the rearmost c.g. location. Results of a stability analysis indicated that the wing would have to be twisted and cambered to produce a positive C_{M_0} of about .020.

Analytical Methods

Skin Friction and Roughness Drag.- The skin-friction drag was calculated using Sommer and Short T' method of reference 6. The skin-friction drag coefficient was computed by representing the various configuration components by appropriate wetted areas and reference lengths and assuming smooth flat-plate, adiabatic-wall, boundary-layer conditions. The drag is computed for a given Mach number and altitude on a standard hot day. Transition from laminar to turbulent is assumed to occur at the

leading edge of each component. Configuration components, which exhibit significant variations in reference length such as the wing, were further subdivided into strips for a more accurate determination of friction drag.

A roughness drag increment was also included in the drag polars. Based on estimates from previous studies (refs. 3 and 5), the roughness drag was estimated to be 5 to 6 percent of the skin-friction drag.

Wave Drag.- The far-field wave-drag program of reference 8 was used to calculate wave drag. The program utilizes the supersonic area-rule concept to compute the zero-lift wave-drag of arbitrary configurations. Equivalent bodies of revolution are calculated by passing a number of cutting planes inclined at the Mach angle through the configuration at several different azimuth angles. The wave drag of each equivalent body is determined from the Von-Karman slender-body theory, which relates the wave drag to the freestream conditions and the equivalent body area distribution. The discrete equivalent-body wave-drag values are then integrated around the configuration and averaged to obtain overall wave drag.

Lift Analysis.- The wing lifting characteristics, drag-due-to-lift, and pitching-moment behavior were computed using the linear theory methods of reference 9 and computer codes described in references 10-13. The method breaks an arbitrary planform arrangement into a mosaic of "Mach Box" rectilinear elements which are assumed to lie to the horizontal plane. These grid elements are then employed to evaluate numerically the linear-theory integral equation which relates the lifting pressure at a given field point to the wing surface slopes in the region of influence of that field point. The overall force coefficients for the camber surface at incidence are obtained by integrating the computed pressure distribution over the wing surface. This solution is combined using a superposition technique with the flat-wing coefficients per unit angle of attack to obtain the variation of the force coefficient with angle of attack.

The nacelle-on-wing interference effects, which are calculated utilizing linear theory corrected for the presence of finite shocks in the vicinity of the nacelle, are incorporated with the lift, drag-due-to-lift, and pitching-moment characteristics computed with this method.

In addition, the lift analysis program also includes the following features: the effect of fuselage upwash field on the wing canard, the effect of wing downwash of the fuselage lift distribution, and the effect of the wing pressure field acting on the nacelles. For this analysis, the fuselage was modeled as a body of revolution, and the local surface angles of attack of the wing canard were increased by the fuselage upwash values. In summary, the lift, drag-due-to-lift, and pitching-moment analysis of the configuration included the effects of wing-body-canard interference, fuselage upwash on wing canard, and canard downwash on the wing. Also, the effects of nacelle pressure signatures on the wing and attainable leading-edge suction were included.

Wing Design

The next step in the configuration development was to design an efficient wing, and then carefully integrate the wing with the fuselage. Linearized supersonic compressible-flow theory was used with the methods described in references 10, 11, and 16 to design and analyze the wing. As stated in reference 16, great care must be taken when designing highly-swept supersonic wings in order that the theoretical

flow prediction can be expected in real life. Examination of test results have shown that when designing a highly-cambered twisted wing in conjunction with wing thickness and body effects, the following four flow conditions must be avoided: extremely high-suction pressures (large negative C_p's), strong spanwise flow, inboard shock separation, and trailing-edge shock separation.

The first step in designing the wing was to determine the design-lift and pitching-moment characteristics. Analytical study indicated that a design C_{M_0} at .020 was desirable, and that a design cruise lift coefficient of .09 would be adequate. These lift and pitching-moment constraints were applied to four slightly different arrow-wing planform shapes (fig. 1).

Assuming a highly-swept arrow wing with subsonic leading edges, a very small nose radius (sharp L.E.) will cause a severe adverse pressure gradient at low incidence angles resulting in separated vortex flow. If this happens, the experimental drag is much higher than the theoretical drag since all leading-edge thrust is lost. To obtain the potential for low drag on highly-swept wings, leading-edge vortex separation must be avoided. A round leading edge tends to alleviate pressure gradients thereby suppressing the formation of separated flow (refs. 17-19); therefore, the basic airfoil used was a modified NACA 64A series airfoil (ref. 20). The airfoil was modified to have a "flat-top" region on the upper-surface center section. Details of this modification are discussed in reference 3. Maximum section thickness of any part of the wing is 3 percent.

To avoid an excessive negative pressure coefficient, a pressure limit constraint of 0.7 $C_{p_{vac}}$ was incorporated into the wing design routine. To avoid strong spanwise flow, it is necessary to prohibit the development of increasing negative pressures near the wing tip. Theoretical studies indicate that wing-thickness pressures which build up near the wing tip are a major contributor to tip pressures. Fortunately, wing outboard thickness pressures are insensitive to changes in airfoil shape or thickness in the inboard wing; therefore, the wing tip must be kept thin to limit spanwise flow.

Inboard shock separation must be avoided. This shock is associated with the flow near the wing leading-edge junction with the body. Due to the reduction in fuselage cross-sectional area caused by supersonic area ruling, the local flow on the upper surface of the wing must be directed inward, then the flow must turn to run parallel to the local body surface. The subsequent turning of the flow causes compression waves, which may coalesce and form a shock wave which is swept aft at approximately the local flow Mach angle. If the required turning angle is large enough, the shock may be strong enough to separate the boundary layer. Normally, a limit is put on the minimum allowable pressure coefficient in the region of the wing-body junction to prevent inboard shock separation. This limit depends on wing sweep, local body curvature, and freestream Mach number. For the configuration studied here, the local body curvature tapers inward very gradually, and then remains relatively constant as the fuselage area tapers to zero. As a result, inboard shock separation is not anticipated.

Wing planforms having a supersonic trailing edge develop a trailing-edge shock across which the upper-surface pressures adjust to approximately freestream static pressure. The strength of the trailing-edge shock is directly associated with the upper-surface pressure and upper-surface pressure gradients at the trailing edge. In order to prevent trailing-edge separation, a constraint must be put on the minimum negative C_p and on the minimum adverse pressure gradient, $\partial C_p/\partial X$. The

minimum C_p had already been limited to .7 $c_{p_{vac}}$, and $\partial C_p/\partial X$ was limited to 0.005/ft.

A final design consideration is that of wing root camber. The design code, when used without constraints, will provide a theoretically optimum wing (refs. 21-22) which has infinite camber at the root. Since this is obviously not feasible, the root camber must be constrained in order that the wing may be integrated with the fuselage. Zero camber at the root would be undesirable since induced drag efficiency would suffer. Upon studying realistic camber distributions of supersonic fuselages, it was determined that a maximum root camber of 15 percent would be tolerable.

The actual design of the wing (determination of wing twist and camber) was done using the computer codes and methods of references 9-13. These codes, which allow for the direct application of the previously discussed design constraints, iterate for the required twist and camber distributions. The loading for determining twist and camber is optimized from a predefined set of component loadings used in conjunction with a series of configuration dependent loadings for fuselage upwash, fuselage buoyancy, and nacelle buoyancy. Previous studies (ref. 3) have indicated that the inclusion of uniform and linear spanwise component loadings produced unmanageable wing root camber; therefore, the basic component loadings defined in the wing design program have been replaced with a series of apex loadings defined in reference 23. Excluding the uniform and linear spanwise loadings when using the apex loadings resulted in a satisfactory camber distribution.

Attempts to design the wing in the presence of the arbitrary cross-section fuselage proved unsuccessful; however, when the fuselage was modeled as an equivalent body of revolution with circular cross sections, the thickness pressures and upwash field could be computed and used in designing the isolated wing. Nacelle effects were not included in the design of the wing.

The wing-design code was used to develop twist and camber distributions for the four wing planform surfaces. Examination of the drag-due-to-lift factors, minimum zero lift induced drag coefficients and aerodynamic center locations indicated planform number 2 to be the most effective.

Wing-Body Integration

The fuselage was integrated with the wing maintaining, as closely as possible, the optimum wing aerodynamic characteristics by the use of the procedures used in references 17 and 24. These procedures require that the change in cross-sectional area with length, $\Delta A/\Delta X$, above and below the wing camber surface be held equal for each fuselage station. This requirement was approximated when the fuselage was area ruled for minimum wave drag. The end result is a highly-cambered arbitrarily shaped fuselage which is elliptical in cross section and has varying cross-sectional area in the longitudinal direction.

Canard Design

Five different canard geometries (fig. 2) were evaluated. Each canard surface was sized to provide sufficient control power for rotation, takeoff, approach, and landing. The sizing was done based on estimated c.g. locations. A comparison of aerodynamic characteristics of the canards is shown in figure 3. Figure 3(a) shows the wetted area of each canard surface, and figure 3(b) shows the wing-body-canard

drag-due-to-lift factor. In analyzing the induced drag of the entire configuration, the fuselage was modeled as a body of revolution having circular cross sections.

Figure 3 (b) shows that the planforms with both leading and trailing edges swept rearward (variants A, C and E) provided minimum drag due to lift. In some cases, the induced drag was less with the canard than with no canard. This indicates favorable interference between the body and lifting surfaces. Figure 3(c) shows the skin-friction drag, D/q, of the canard surfaces computed using references 10-13. The values of D/q do not follow the same pattern as the wetted areas (fig. 3(a)) because of the different chord Reynolds numbers.

Finally, figure 3(d) shows the overall performance of the five surfaces by presenting the difference in total drag between the canard configurations and the no-canard configurations while operating at a cruise C_L of 0.10 (M = 2.62, h = 58,000 ft). The total drag includes wave drag, roughness drag, induced drag, and skin-friction drag. It can be observed that all surfaces provide favorable drag decreases in spite of the additional viscous drag of the canard surfaces. From figure 3(b), it can be seen that two of the surfaces have higher drag due to lift than the no-canard case, however, these surfaces still show a net reduction in drag because the zero-lift induced drag of these two surfaces is lower than that of the remaining three. Based on figure 3(d), canard variant E was selected for the configuration.

Wave Drag

The computer code of reference 8 was used to evaluate the wave drag of the configuration. In the wave-drag analysis, 60 longitudinal cuts and 16 angular cuts were used in calculating wave drag. Area-ruling the fuselage to have minimum wave drag at cruise was a tedious process; however, eventually, a nearly optimum wave drag coefficient of 14.91 counts was obtained. Figure 4 presents the normal cross-sectional area of the configuration broken down into separate components. Although the canard area protrudes noticeably in the figure, the integrated average equivalent body produces an almost bell-shaped area curve at Mach 2.62.

Final Configuration

A final lift and balance analysis of the configuration showed that slightly more positive pitching moment would be required at zero lift. Through trial and error, the cranked tip of the wing was twisted slightly to increase C_{M_0}. The pressure distribution was examined to insure that the limiting pressure constraints had not been violated. The wing twist and maximum thickness distribution are shown in figures 5 and 6. Figure 7 shows the camber distribution of the wing, and figure 8 shows the top and side views of the overall configuration.

Interior Arrangement

Figure 9 shows a planview of the interior arrangement. The interior is based on the same methodology as the AST-205 (ref. 5). Tourist class seating is provided for 290 passengers plus crew. The seats are advanced technology, nonreclining, lightweight versions with 30-inch seat pitch. The seating varies from three to six

abreast. Volume is allotted in the forward cabin for lavatories and galley. A lavatory is provided for every 70 passengers. The main wing carry-through spars are located aft of the passenger cabin. Baggage is limited to 5 cubic feet per passenger and is stored in the thick wing-root area adjacent to the cabin. Underfloor volume is used for hydraulic lines, electrical cables, and environmental systems.

Airplane subsystems and environmental control, hydraulic, electrical, electronic, and avionic systems were assumed to be based on improved technology requiring minimum volume and were located in available space. All fuel is carried in the wing center structure with the exception of two fuselage tanks. The fuel system contains eighteen fuel cells and is designed so that fuel can be pumped and circulated for aid in structural cooling and for c.g. management.

PROPULSION SYSTEM

The engines selected for this configuration are the General Electric GE21/J11-B14a. This engine is an augmented, double-bypass variable-cycle engine which was designed for cruise at Mach 2.62 at an altitude of 65,000 feet on standard day +8°C. The baseline engine design is based on 1985 technology. Installed engine performance data at standard day +8°C and standard day +10°C atmospheric conditions are provided.

The NASA-Ames "P" inlet (ref. 25) was installed on the engine, and the engine performance was adjusted for the installation effects of inlet recovery, service airbleed, mechanical sound suppressor, and power extraction, as well as afterbody, inlet spillage, and inlet bypass drags. Nacelle geometric data necessary to estimate nacelle drag and weight for the inlet and engine combination were also developed.

Baseline Engine

In its basic configuration, the engine has a design overall pressure ratio of 13.5 and a bypass ratio of 0.25. With the sound suppressor deployed, it develops a maximum sea-level static takeoff thrust of 61,271 lbf for a standard +8°C atmosphere with an airflow rate of 843 lbm/sec. The engine is equipped with a low temperature (1900°F) augmentor. The exhaust system consists of an annular translating-plug nozzle with a thrust reverser and mechanical sound suppressor installed in the outer stream of the nozzle. Weight of the baseline engine is 14,270 lbm including the nozzles, thrust reverser, and mechanical sound suppressor.

Engine Sizing

The baseline engine was resized using relative thrust where relative thrust is the ratio of the desired thrust to the baseline engine thrust. Fuel flow, gross thrust, ram drag, and engine airflow are scaled in direct proportion to relative thrust. Engine weight varies as the 1.2 power of relative thrust, and the length and diameter vary as the square root of relative thrust.

The external configuration and envelope of the required engine is shown in figure 10. For the baseline configuration, the engines were resized to 48,000 pounds thrust each. This represents a T/W of .30 for an estimated gross weight of 640,000 lbf. Weight of this engine is 10,982 lbm which includes the nozzle, thrust reverser, and mechanical sound suppressor.

Nacelle and Inlet

The four engines are located at the rear of the fuselage, clustered together in a rectangular "box-type" nacelle. The inlet used on the nacelle is th NASA-Ames "P" inlet (ref. 25). It is an axisymmetric mixed-compression design with a translating centerbody sized for supersonic cruise conditions. Allowance was made in the inlet design to provide 2 percent of the inlet system airflow for nacelle cooling and ventilation. Inlet performance is shown in figure 11.

Propulsive Performance

Installed engine performance presented in this document includes the effects of inlet pressure recovery, compressor airbleed, power extraction and, at takeoff conditions, the mechanical sound suppressor. The effects of afterbody drag from the customer-connect point to the end of the exhaust nozzle plug are also included in the installed performance. At all engine operating conditions, engine performance has also been adjusted for the effects of inlet spillage, bleed, and bypass drags. Nacelle skin friction, interference, and wave drag are accounted for in the aircraft drag polars. It is important to realize that all SFC's for the baseline engine have been decreased by 8 percent to represent more advanced 1995 technology.

The installed engine performance is based on standard atmospheric conditions, inlet total pressure recovery obtained from reference 21, and fuel with a lower heating value of 18,400 btu/lbm. Engine airbleed of 2 lbm/sec per engine during idle at 20,000 feet and below, and 1 lbm/sec at all other operating conditions, was assumed to account for aircraft service air requirements. Power extraction of 200 HP per engine was also included to meet the aircraft system power requirements.

Mechanical Sound Suppressor

The mechanical sound suppressor employed on the GE21/J11-B14a engine is a 20 shallow-chute outerstream design. This suppressor is estimated by General Electric to provide 4 db of suppression at all conditions while deployed. Estimated weight of the sound suppressor for the baseline engine is 720 lbm.

MASS PROPERTIES

Baseline Configuration

The methods used to estimate the weights are consistent with the methods used in the AST-205 studies (ref. 5). Several new weight reduction concepts which were implemented in the AST-205 studies were also implemented in the CST-11 studies. These concepts place emphasis on airframe weight reduction through the use of 1985 level superplastic-formed diffusion-bonded (SPF/DF) titanium technology. This technology was applied to all primary and secondary airframe structures. The wing and aerodynamic surfaces are constructed of SPF/DB titanium skin/core sandwich cover panels with SPF/DB titanium substructure. The fuselage structure consists of SPF/DB titanium skin/core sandwich panel covering with integral frames and crack stoppers. The engine nacelles are constructed of SPF/DB titanium skin/core sandwich panels with integral frames. The landing gear consists of two-strut main and single-strut nose-gear structure of high strength steel. Finally, the engines are variable-cycle

turbofan engines with dimensions, weight, and airflow scaled from the General Electric GE21/J11-B14a baseline engine.

Weight and Balance

The weight and balance analysis consisted of using the selected configuration geometry as input and performing a semi-detailed allocation of mass by major aircraft components, systems, and loading conditions.

Combinations of fuel utilization and transfer sequencing were used to determine the most forward and aft attainable c.g. boundaries. These limiting boundaries, expressed as a percent of the mean aerodynamic chord are as follows:

Flight Condition	Forward Limit (% MAC)	Aft Limit (% MAC)
Takeoff	30.2	39.0
Begin Cruise	26.0	39.6
Landing	14.6	25.3

The optimum c.g. location at the beginning of cruise is 34.4-percent MAC; however, as the end of cruise segment is approached, the c.g. must move forward to the 27.3-percent MAC position. At this c.g. position, a small trim-drag penalty of 1.5 percent of the total drag must be incurred. Trailing-edge flaps, as well as canard deflection, are used to trim the airplane at this c.g. position. Details of the trim characteristics will be discussed in a subsequent section.

LOW-SPEED AERODYNAMICS

The low-speed drag polars for this configuration were not computed but were assumed to be typical of the highly-swept arrow-wing supersonic transport configurations discussed in references 2 to 5.

HIGH-SPEED AERODYNAMICS

Supersonic drag polars for Mach numbers ranging from 1.05 to 2.62 were established utilizing various analytical methods and computer programs. Although primary emphasis was focused on the Mach 2.62 cruise aerodynamics, trim and control capability were examined over the entire supersonic Mach number range. The computed supersonic drag polars consist of skin-friction drag, roughness drag, wave drag, and drag-due-to-lift. Figure 12 is a plot of the zero-lift wave-drag coefficient as a function of Mach number and figure 13 is a plot of the friction and roughness drag coefficients as a function of Mach number.

Untrimmed Lift and Drag Performance

Figure 14 shows the untrimmed lift-drag performance of the configuration without the canard and with a canard at incidence angles of 0 and 3.4 degrees.

For Mach 2.62 cruise at 55,000 feet altitude, a maximum L/D of 11.04 occurs when the canard is deflected 3.4 degrees (trailing edge down). At 0 degrees canard incidence, the interference is not as favorable and the maximum L/D is reduced to 10.68, a reduction of 3.3 percent. The no-canard configuration shows about the same

maximum L/D as the 0 degree incidence canard; however, its maximum L/D occurs at a C_L which is significantly greater than the cruise C_L of 0.075. Drag polars are shown in figure 15. It can be seen that the zero-lift drag of the degree incidence canard is much higher than the other two cases. This is because the wing-reference plane is at about -1 degree angle of attack when the wing is operating at zero lift; therefore, the canard at 0 incidence must carry a download which requires more lift from the wing.

Figure 16 shows the maximum L/D as a function of canard incidence. Assuming that the airplane can be trimmed at any canard incidence angle through fuel management, it appears that the optimum incidence angle is 3.4 degrees for Mach 2.62 cruise at 55,000-feet altitude. During 65 percent of the cruise segment, the c.g. can be located at the optimum point of 34.4-percent MAC; however, during the latter part of cruise, the c.g. must move forward, requiring a maximum incidence angle of 4.9 degrees. At this c.g. position, the wing trailing-edge flaps are deflected slightly to provide more efficient trim.

Trimmed Lift and Drag Performance

Figures 17 and 18 show the trimmed-cruise lift and drag performance for both the beginning and end of the cruise segment. At the beginning of cruise and throughout 60 percent of the cruise segment, the aircraft can be trimmed at the optimum c.g. location through fuel management. This corresponds to 34.4-percent MAC. With a static margin of 20.6 percent, a canard incidence of 3.4 degrees, and a trim C_L of .078.

Approaching the end of cruise, the c.g. moves forward to the 27.3-percent MAC position. At this point, the airplane is trimmed using both the canard and trailing-edge flaps. The canard is deflected 4.9 degrees, while the inboard flaps are deflected -2 degrees (upward) and the outboard flaperons are deflected -4 degrees. This results in a minimum trim drag penalty of 1.5-percent increase of the total drag.

Figure 19 shows the attainable leading-edge suction available at Mach 2.62 cruise. Since the wing has a subsonic leading edge over 71 percent of its span, there is the potential of a slight drag reduction during cruise; thus, attainable leading-edge suction was used in computing the drag polars. A breakdown of the total drag at a C_L of 0.10 (C_L for L/D_{MAX}) is shown in bar-chart form in figure 20.

Figure 21 presents the pitching-moment characteristics for the forward and aft c.g. locations. The pitching moment for the no-canard configuration is also shown. These forward and aft c.g. locations correspond to the beginning-of-cruise and end-of-cruise conditions. It can be seen that with the c.g. position held constant, the addition of the canard has a destabilizing effect on stability; however, the stability still remains positive. As the c.g. moves forward (approaching the end-of-cruise position), the stability increases. Both pitching-moment curves representing cruise are trimmed at a C_L of .078, and the static margin for these two cases varies from 20 to 27 percent.

The configuration can be trimmed for minimum trim drag throughout 65 percent of cruise segment. For the remaining 35 percent of cruise segment, the trim-drag penalties are small (approx. 1.4-percent maximum increase in total drag).

Also, during supersonic cruise, c.g. may travel from 18.4 to 27.5 percent positive static margin. Fully-loaded, zero-fuel c.g. during landing is 29.8-percent static margin.

SIZING AND MISSION ANALYSIS

Mission

The design payload was selected to be 290 passengers plus baggage, resulting in a payload weight of 60,610 lbf. The design range was 6,000 nautical miles and the design cruise Mach number was 2.7 (Mach 2.62 on a standard +8°C day temperature). Operational design requirements included a balanced takeoff field length not to exceed 10,000 feet (performed at standard +10°C day temperature) and an approach speed not to exceed 155 knots.

Adequate fuel reserves are important. Reserve fuel requirements are computed based on the following conditions: one missed approach and go-around, 250 nautical miles to alternate airport to be flown at best altitude and Mach number, 30 minutes in holding pattern to be flown at best altitude and Mach number, and headwinds or off-nominal operation equal to 5 percent of trip fuel. These reserves are based on proposed fuel reserve allowances for supersonic fleet air carrier operations. The allowances are based on the requirements contained in Federal Air Regulations, Part 121 (FAR 121), Sections 121.645 and 121.647, modified to include recommendations from the Air Transport Association (ATA).

The 30-minute holding pattern is flown at Mach 0.8 at 35,000 feet altitude. The holding conditions were determined after a matrix of hold altitudes and Mach numbers were evaluated to determine an optimum hold condition. The subsonic cruise to the alternate airport is flown at the best subsonic Brequet factor.

Figure 22 shows the mission profile used in this study. The supersonic cruise segment is flown at maximum Brequet factor; therefore, as fuel is burned off and the aircraft becomes lighter, it must climb to maintain maximum Brequet factor.

To evaluate the mission performance, the configuration was "flown" via the computer program in accordance with the selected mission profile. For each segment of the profile, the program determined enroute details such as thrust and fuel flow required, altitude, speed, and end point times of the segments. The profile used in this study consisted of the following segments:

Taxi-out - Estimated fuel for 10 minutes warm-up and taxi-out;

Takeoff - Velocity at rotation is 165 knots, C_L at rotation is .75, balanced field length not to exceed 10,000 ft;

Climb and Accelerate;

Cruise - Cruise begins at altitude which will yield maximum Brequet factor and the maximum Brequet factor is maintained throughout the cruise segment;

Descent - Descent is performed at L/D_{MAX} with the thrust assumed to be zero and fuel flow assumed as 6 percent of maximum at the corresponding Mach numbers and altitudes throughout the descent;

Taxi-in - Fuel taken out of the reserves at destination, with no additional time allocated.

Configuration Sizing

Configuration sizing and performance evaluations were accomplished using the Aircraft Sizing and Performance (ASP) Program of reference 14. Before any sizing was done, the data base representing the baseline aircraft was input. Since the program does not synthesize any aerodynamic, propulsion, or weight data, this information was also input with the baseline data. The sizing process requires an array of values for wing loading and thrust-weight ratio that represent a range of combinations applicable to the configuration and mission studies. With these inputs accomplished, the sizing procedure began. The program selects the first combination of W/S and T/W, and then iterates the takeoff gross weight until the design range is met. During iterations, the wing area and engine thrust vary with gross weight while W/S and T/W remain constant. The baseline weights are scaled with changing takeoff gross weight. This process is then repeated for the various remaining combinations of W/S and T/W. During sizing, thrust-weight ratios varying from .20 to .40 were evaluated. The principal factors affecting power plant sizing are takeoff field length, safety regulations applicable to takeoff (which include balanced field length and maintaining a given minimum rate of climb with one engine inoperative), adequate power for acceleration to desired cruise speed, and cruise efficiency.

After the sizing procedure was completed, the results were used to prepare a "thumbprint" plot (fig. 23). One primary advantage of the "thumbprint" plot is the ability to choose quickly the candidate aircraft which has the best potential for achieving the design mission goals in terms of the essential sizing parameters. From figure 23, it can be seen that the baseline concept was very close to the constrained optimum with respect to wing loading and thrust-to-weight ratio; therefore, the wing area and engine size of the baseline configuration was not altered. The design gross weight had to be slightly adjusted in order to meet the design range of 6,000 nautical miles; therefore, the weights for the baseline had to be updated based on the new gross weight. Since the wing area and engine size of the updated baseline did not change, there was no need to regenerate the aerodynamics.

The updated configuration has the following characteristics: a design gross weight of 687,200 lbf; a wing loading of 69.8 lbf/ft^2; and a thrust-weight ratio of .278 installed, sea level, on a standard +10°C day. Geometric characteristics of the configuration are shown in Table I. A numerical model of the configuration in the "wave-drag" format (ref. 8) is given in Table II. The engines are 4 General Electric GE21/J11-B14a variable-cycle engines of 48,000-pounds maximum thrust each. SFC's of 1985 technology baseline were decreased by 8 percent to represent approximately 1995 technology. The results of the mission performance are summarized in Table III. Since this aircraft was designed to have excess fuel volume available over that required for the 6,000 nautical miles, 100-percent payload mission, it has the capability to offload payload in exchange for fuel. At 60-percent payload, a range of 7,000 nautical miles can be obtained (fig. 24). The climb cruise and descent altitude profiles as a function of Mach number are shown in figure 25. A group weight summary for the final configuration is shown in Table IV. The tabulated data is also shown in bar-chart form together with major component masses as a percentage of the total (fig. 26).

Figure 27 shows the c.g. envelope. Center-of-gravity locations in the region aft of 41-percent MAC, which is coincident with the main landing gear, would be unacceptable for ground operations and would require fuel loading restrictions.

CONCLUDING REMARKS

The most significant result of this study is that a significantly improved trimmed-cruise maximum lift-drag ratio of 11.04 can be obtained at Mach 2.62, and 55,000 feet.

The configuration was sized to carry 290 passengers 6,000 nautical miles nonstop. As an alternate mission, payload can be off-loaded for additional fuel capacity. At 60-percent payload, a range of 7,000 nautical miles can be obtained. The final configuration has a maximum takeoff gross weight of 687,200 pounds, a wing loading of 69.8 lbf/ft^2, and a thrust-weight ratio of .278.

REFERENCES

1. Rowe, W. T.: Technology Status for an Advanced Technology Supersonic Transport. SAE Paper No. 820955, 1983.

2. Baber, Hal T., Jr.: Characteristics of the Advanced Supersonic Technology AST-105-1 Configured for Transpacific Range with Pratt and Whitney Aircraft Variable Stream Control Engines. NASA TM 78818, 1979.

3. Walkley, Kenneth B.; and Martin, Glen L.: Aerodynamic Design and Analysis of the AST-200 Supersonic Transport Configuration Concept. NASA CR-159051, 1979.

4. Martin, Glenn L.; and Walkley, Kenneth B.: Aerodynamic Design and Analysis of the AST-204, -205, and -206 Blended Wing-Fuselage Supersonic Transport Configuration Concepts. NASA CR-195223, 1980.

5. Walkley, K. B.; Espil, G. J.; Lovell, W. A.; Martin, G. L.; and Swanson, E. E.: Concept Development of a Mach 2.7 Advanced Technology Transport Employing Wing Fuselage Blending. NASA CR-165739, 1981.

6. Sommer, Simon C.; and Short, Barbara J.: Free Flight Measurements of Turbulent Boundary Layer Skin Friction in the Presence of Severe Aerodynamic Heating at Mach Numbers from 2.8 to 7.0. NACA TN 3391, 1955.

7. Harris, Roy V., Jr.: An Analysis and Correlation of Aircraft Wave Drag. NASA TM X-947, 1964.

8. Craidon, Charlotte B.: User's Guide for a Computer Program for Calculating the Zero-Lift Wave Drag of Complex Aircraft Configurations. NASA TM 85670, 1984.

9. Carlson, Harry W.; and Miller, David S.: Numerical Methods for the Design and Analysis of Wings at Supersonic Speeds. NASA TN D-7713, 1974.

10. Middleton, W. D.; and Lundry, J. L.: A Computational System for Aerodynamic Design and Analysis of Supersonic Aircraft. Part 1 - General Description and Theoretical Development. NASA CR-2715, 1976.

11. Middleton, W. D.; Lundry, J. L.; and Coleman, R. G.: A Computational System for Aerodynamic Design and Analysis of Supersonic Aircraft. Part 2 - User's Manual. NASA CR-2716, 1976.

12. Middleton, W. D.; Lundry, J. L.; and Coleman, R. G.: A Computational System for Aerodynamic Design and Analysis of Supersonic Aircraft. Part 3 - Computer Program Description. NASA CR-2717, 1976.

13. Middleton, W. D.; Lundry, J. L.; and Coleman, R. G.: A Computational System for Aerodynamic Design and Analysis of Supersonic Aircraft, Part 4 - Test Cases. NASA CR-2718, 1976.

14. Fetterman, D. E.: Preliminary Sizing and Performance Evaluation of Supersonic Aircraft. NASA TM X-73936, 1976.

15. Ferri, Antonio: Possibilities and Goals for the Future SST. J. Aircraft, Vol. 12, No. 12, December 1975.

16. Kulfan, R. M.; and Sigalla, A.: Real Flow Limitations in Supersonic Airplane Design. AIAA Paper 78-147, 1978.

17. Robins, A. Warner; Carlson, Harry W.; and Mack, Robert J.: Supersonic Wings with Significant Leading-Edge Thrust at Cruise. NASA TP-1632, 1980.

18. Mack, Robert J.: A Numerical Method for Evaluation and Utilization of Supersonic Nacelle-Wing Interference. NASA TM D-5057, 1969.

19. Carlson, Harry W.; Mack, Robert J.; and Barger, Raymond L.: Estimation of Attainable Leading-Edge Thrust for Wings at Subsonic and Supersonic Speeds. NASA TP-1500, 1979.

20. Patterson, Elizabeth W.; and Braslow, Albert L.: Ordinates and Theoretical Pressure-Distribution Data for NACA 6- and 6A-Series Airfoil Sections with Thicknesses from 2 to 21 and from 1 to 15 Percent Chord, Respectively. NASA TR R-84, 1961.

21. Baals, Donald D.; Robins, A. Warner; and Harris, Roy V., Jr.: Aerodynamic Design Integration of Supersonic Aircraft. AIAA Paper 68-1018, 1968.

22. Robins, A. Warner; Morris, Odell A.; and Harris, Roy V., Jr.: Recent Research Results in the Aerodynamics of Supersonic Vehicles. J. Aircraft, Vol. 3, No. 6, November-December 1966.

23. Miller, Davis S.; and Schemensky, Roy T.: Design Study Results of a Supersonic Cruise Fighter Wing. AIAA Paper 79-0062, 1979.

24. Dollyhigh, Samuel M.; Morris, Odell A.; and Adams, Mary S.: Experimental Effects of Fuselage Camber on Longitudinal Aerodynamic Characteristics of a Series of Wing-Fuselage Configurations at a Mach Number of 1.41. NASA TM X-3411, 1976.

25. Koncsek, J. L.; and Syberg, J.: Transonic and Supersonic Test of a Mach 2.65 Mixed Compression Axisymmetric Intake. NASA CR-1977, 1972.

TABLE I.- CONFIGURATION GEOMETRIC CHARACTERISTICS

Geometry	Wing	Canard	Vertical Fin
Gross area, ft^2	9900.0	601.5	300.0
Gross MAC, ft	98.80	13.75	15.00
Reference area, ft^2	9900.0	601.5	300.0
Reference MAC, ft	98.8	13.75	15.00
Span, ft	130.0	44.0	-
Aspect ratio	1.707	3.220	1.334
Sweep, Λ_{LE}	74°, 58°	43°	67°
Root chord, ft	143.5	19.5	24.0
Tip chord, ft	24.0	8.0	6.0
Root t/c, %	3.024	3.0	3.0
Tip t/c, %	3.0	3.0	3.0
Taper ratio	-	0.41	0.25
Volume coefficient (based on takeoff c.g.)	-	0.100	0.029

TABLE II.- CONFIGURATION NUMERICAL MODEL

```
CSTLZ11....   CANARD ARROW-WING SUPERSONIC TRANSPORT CONFIGURATION
  1  1  1  1  1  1     9 20  1 10 20                    2 20  1 10  1 10
9900.  98.800 190.000                                                REFA
.0     .500   1.00   1.5    2.50    5.0   10.0   15.0   20.0    30.    XAF 10
 40.    50.    60.    70.    75.    80.    85.    90.    95.   100.    XAF 20
 98.5    5.0   0.0    143.5                                          WXYZ  1
115.0   10.0    -4.00  127.0                                         WXYZ  2
150.0   20.0    -9.93  101.0                                         WXYZ  3
184.0   30.0   -12.13   77.0                                         WXYZ  4
219.0   40.0   -13.93   51.5                                         WXYZ  5
240.0   46.0   -14.81   37.0                                         WXYZ  6
249.5   52.0   -14.87   33.0                                         WXYZ  7
259.0   58.0   -14.97   29.0                                         WXYZ  8
270.0   65.0   -15.07   24.0                                         WXYZ  9
  0.000  -.020  -.039  -.059  -.099  -.197  -.798 -1.665 -2.531 -4.542  TZ  1
 -6.571 -8.475-10.182-11.667-12.299-12.930-13.456-13.981-14.397-14.814  TZ  1
  0.000  -.001  -.001  -.002  -.003  -.007  -.319  -.833 -1.347 -2.588  TZ  2
 -3.894 -5.190 -6.443 -7.632 -8.196 -8.760 -9.292 -9.824-10.322-10.819  TZ  2
  0.000   .024   .048   .073   .121   .242   .262   .147   .031  -.369  TZ  3
  -.869 -1.434 -2.047 -2.706 -3.055 -3.403 -3.770 -4.137 -4.513 -4.889  TZ  3
  0.000   .025   .050   .075   .126   .252   .354   .368   .381   .255  TZ  4
   .026  -.285  -.661 -1.097 -1.342 -1.586 -1.852 -2.118 -2.400 -2.683  TZ  4
  0.000   .019   .037   .055   .092   .185   .331   .393   .454   .464  TZ  5
   .394   .260   .088  -.124  -.243  -.363  -.490  -.618  -.751  -.884  TZ  5
  0.000  0.000  0.000  0.000  0.000  0.000  0.000  0.000  0.000  0.000  TZ  6
  0.000  0.000  0.000  0.000  0.000  0.000  0.000  0.000  0.000  0.000  TZ  6
  0.000  0.000  -.001  -.001  -.001  -.003  -.006  -.009  -.012  -.017  TZ  7
  -.023  -.029  -.035  -.040  -.043  -.046  -.049  -.052  -.055  -.058  TZ  7
  0.000  -.001  -.002  -.002  -.004  -.008  -.015  -.023  -.030  -.046  TZ  8
  -.061  -.076  -.091  -.106  -.114  -.121  -.129  -.137  -.144  -.152  TZ  8
```

```
 0.000  -.001  -.003  -.004  -.006  -.013  -.025  -.038  -.050  -.075  TZ  9
 -.101  -.126  -.151  -.176  -.189  -.201  -.214  -.226  -.239  -.251  TZ  9
0.      .237   .333   .405   .514   .712   .978  1.157  1.292  1.461    WORD1.1
1.512  1.512  1.512  1.192  1.003  0.806  0.606  0.406  0.208  0.000   WORD1.2
0.      .225   .316   .386   .490   .679   .931  1.103  1.232  1.392    WORD2.1
1.441  1.441  1.437  1.132  0.953  0.765  0.576  0.385  0.197  0.000   WORD2.2
 0.000   .216   .304   .370   .470   .651   .894  1.059  1.182  1.336  WORD3.1
 1.383  1.383  1.341  1.056   .889   .714   .537   .360   .184  0.000  WORD3.2
 0.000   .208   .294   .358   .455   .631   .866  1.025  1.144  1.293  WORD4.1
 1.338  1.338  1.277  1.006   .848   .681   .512   .343   .175  0.000  WORD4.2
 0.000   .200   .283   .344   .438   .607   .833   .987  1.101  1.244  WORD5.1
 1.287  1.287  1.186   .935   .788   .633   .476   .319   .163  0.000  WORD5.2
 0.000   .029   .059   .088   .146   .285   .541   .766   .961  1.261  WORD6.1
 1.440  1.500  1.440  1.261  1.126   .961   .766   .541   .285  0.000  WORD6.2
 0.000   .029   .059   .088   .146   .285   .541   .766   .961  1.261  WORD7.1
 1.440  1.500  1.440  1.261  1.126   .961   .766   .541   .285  0.000  WORD7.2
 0.000   .029   .059   .088   .146   .285   .541   .766   .961  1.261  WORD8.1
 1.440  1.500  1.440  1.261  1.126   .961   .766   .541   .285  0.000  WORD8.2
 0.000   .029   .059   .088   .146   .285   .541   .766   .961  1.261  WORD9.1
 1.440  1.500  1.440  1.261  1.126   .961   .766   .541   .285  0.000  WORD9.2
-20.   00.0   20.    30.    40.    50.0   60.0   70.0    80.0   90.0    XFUS 10
100.0  110.0  120.0  130.0  140.0  150.0  170.0  190.0   212.9  242.0   XFUS 20
   0.00   0.00   0.00   0.00   0.00   0.00   0.00   0.00   0.00   0.00
   6.00   6.00   6.00   6.00   6.00   6.00   6.00   6.00   6.00   6.00
   0.00    .90   2.04   2.52   3.00   3.00   2.46   1.56    .90   0.00
   4.47   4.52   4.83   5.10   5.82   6.18   6.95   7.40   7.51   7.53
   0.00   1.20   2.72   3.36   4.00   4.00   3.28   2.08   1.20   0.00
   2.93   3.02   3.63   4.15   5.55   6.25   7.74   8.61   8.83   8.87
   0.00   1.43   3.23   3.99   4.75   4.75   3.90   2.47   1.43   0.00
   2.07   2.17   2.87   3.48   5.10   5.90   7.62   8.63   8.88   8.93
   0.00   1.50   3.40   4.20   5.00   5.00   4.10   2.60   1.50   0.00
   1.45   1.56   2.33   3.00   4.76   5.64   7.51   8.62   8.89   8.95
   0.00   1.56   3.54   4.37   5.20   5.20   4.26   2.70   1.56   0.00
    .42    .54   1.40   2.14   4.11   5.09   7.18   8.41   8.72   8.78
   0.00   1.61   3.64   4.49   5.35   5.35   4.39   2.78   1.61   0.00
```

```
  -.39   -.26    .65   1.42   3.48   4.52   6.71   8.00   8.32   8.39
  0.00   1.67   3.77   4.66   5.55   5.55   4.55   2.89   1.67   0.00
 -1.55  -1.42   -.48    .32   2.46   3.54   5.81   7.15   7.48   7.55
  0.00   1.68   3.81   4.70   5.60   5.60   4.59   2.91   1.68   0.00
 -2.82  -2.67  -1.66   -.79   1.52   2.68   5.14   6.58   6.94   7.02
  0.00   1.71   3.88   4.79   5.70   5.70   4.67   2.96   1.71   0.00
 -4.30  -4.04  -2.97  -2.05    .39   1.61   4.20   5.73   6.11   6.19
  0.00   1.74   3.94   4.87   5.80   5.80   4.76   3.02   1.74   0.00
 -5.50  -5.46  -4.34  -3.39   -.68    .28   3.15   4.74   5.14   5.22
  0.00   1.73   3.91   4.83   5.75   5.75   4.72   2.99   1.73   0.00
 -6.65  -6.49  -5.39  -4.45  -2.58   -.02   2.01   3.58   3.97   4.05
  0.00   1.71   3.88   4.79   5.70   5.70   4.67   2.96   1.71   0.00
 -7.20  -7.05  -6.02  -4.94  -3.86   -.54    .91   2.36   2.72   2.80
  0.00   1.65   3.74   4.62   5.50   5.50   4.51   2.86   1.65   0.00
 -7.68  -7.55  -6.64  -5.89  -5.15  -1.35   -.28    .79   1.11   1.18
  0.00   1.61   3.64   4.49   5.35   5.35   4.39   2.78   1.61   0.00
 -8.48  -7.96  -7.14  -6.65  -6.15  -2.05  -1.26   -.47   -.18   -.12
  0.00   1.56   3.54   4.37   5.20   5.20   4.26   2.70   1.56   0.00
 -9.31  -8.70  -7.93  -7.59  -7.25  -2.95  -2.34  -1.72  -1.45  -1.39
  0.00   1.50   3.40   4.20   5.00   5.00   4.10   2.60   1.50   0.00
-10.90 -10.80 -10.10  -9.89  -9.67  -5.33  -4.87  -4.40  -4.15  -4.10
  0.00   1.50   3.40   4.20   5.00   5.00   4.10   2.60   1.50   0.00
-12.72 -12.64 -12.08 -12.04 -12.00  -8.00  -7.76  -7.52  -7.32  -7.28
  0.00   1.50   3.40   4.20   5.00   5.00   4.10   2.60   0.01   0.00
-13.67 -13.63 -13.35 -13.43 -13.51 -11.11 -11.09 -11.07 -10.96 -10.97
  0.00   1.50   3.40   4.20   5.00   5.00   4.10   2.60   0.01    0.00
-14.41 -14.41 -14.41 -14.40 -14.38 -14.38 -14.36 -14.35 -14.35 -14.35
220.00 3.20   -17.60                                                  PODORG 1
0.     2.     4.     6.     8.     10.    12.    14.    16.    18.    XPOD
20.    22.    24.    26.    28.    30.    31.624 32.    34.    35.963 XPOD
2.578  2.619  2.660  2.702  2.743  2.784  2.825  2.866  2.907  2.949  RPOD
2.990  3.031  3.072  3.113  3.154  3.196  3.229  3.229  3.229  3.229  RPOD
220.00  9.6   -17.60                                                  PODORG 2
0.     2.     4.     6.     8.     10.    12.    14.    16.    18.    XPOD
20.    22.    24.    26.    28.    30.    31.624 32.    34.    35.963 XPOD
```

2.578	2.619	2.660	2.702	2.743	2.784	2.825	2.866	2.907	2.949	RPOD
2.990	3.031	3.072	3.113	3.154	3.196	3.229	3.229	3.229	3.229	RPOD
270.0	65.0	-15.1	24.0	293.0	69.0	-5.1	6.0			V FIN
0.	10.	20.	30.	40.	50.	60.	70.	90.	100.	XFIN
0.	.466	.846	1.138	1.345	1.465	1.498	1.390	.641	0.	FINORD
20.00	5.00	4.00	17.00	36.00	22.00	4.00	8.00			CAN
0.	10.	20.	30.	40.	50.	70.	80.	90.	100.	XCAN
0.0	.553	.948	1.264	1.448	1.5	1.264	.948	.553	0.0	CANORD

TABLE III.- MISSION PERFORMANCE

Mission: Supersonic Cruise at Mach 2.62

Model No.: CST-11

Aircraft characteristics

Design gross weight, lbf	687,200
Operating weight empty, lbf	288,014
Payload - 290 passengers, lbf	47,850
- passenger baggage, lbf	12,760
Total payload weight, lbf	60,610
Wing area - reference, ft^2	9,900
- gross, ft^2	9,900
GE21/J11-B14a engines (4); sea-level static (standard +8°C day) installed thrust per engine, lbf	48,000
Initial installed thrust-to-weight ratio	.278
Initial wing loading - reference, lbf/ft^2	69.7
- gross, lbf/ft^2	69.7

Mission Segment or Condition	Operating weights (lbf)	ΔFuel (lbf)	ΔRange (n.m.)
Ramp gross weight	687,200		
Warm-up and taxi-out		1924.	0
Takeoff gross weight	685,276		
Takeoff segment		3573.	2.2
Begin Ascent	681,703		
Climb & accelerate		64,597.	362.2
Begin cruise	617,106		
Cruise segment		220,110.	5310.0
End cruise	396,996		
Descent & decelerate		3779.	327.6
End descent	393,217		
Landing & taxi-in		-	-
End mission	393,217		
Trip fuel, range		293,983	6,000

TABLE III.- MISSION PERFORMANCE (CONCLUDED)

Reserve fuel breakdown	ΔFuel (lbf)
1. 5% trip fuel	14,740
2. Missed approach	1,085
3. 463 km (250 n.m.) to alternate airport	17,413
4. 30-minute holding at 35,000 ft	11,325
Total reserves	44,563

Cruise conditions:

	Begin cruise	End cruise
Lift coefficient	.0743	.0762
Drag coefficient	.00718	.00759
Lift/drag	10.35	10.03
TSFC, kg/hr/N (lbm/hr/lbf)	1.315	1.347
Altitude	59,100	67,000

Notes:

1. Taxi-in fuel taken out of reserves at destination.

TABLE IV.- GROUP WEIGHT SUMMARY

Item	lbf
Wing	91,228
Canard	2,360
Vertical fin	2,499
Fuselage	52,623
Landing gear	27,514
Nacelle	10,106
Structure total	188,829
Engines	43,928
Thrust reversers	6,077
Miscellaneous systems	1,473
Fuel system - tanks & plumbing	3,966
- insulation	0
Propulsion total	53,971
Surface controls	3,690
Auxiliary power	0
Instruments	720
Hydraulics	3,246
Electrical	3,920
Avionics	2,289
Furnishing and equipment	17,258
Air conditioning	3,884
Anti-icing	360
Systems and equipment total	31,667
Weight empty	277,592
Flight crew and baggage	450
Unusable fuel	2,142
Engine oil	453
Passenger service	7,827
Operating weight	288,014
Passengers, 290	47,850
Passenger baggage	12,780
Zero fuel weight	348,624
Mission fuel	338,576
Takeoff gross weight	687,200

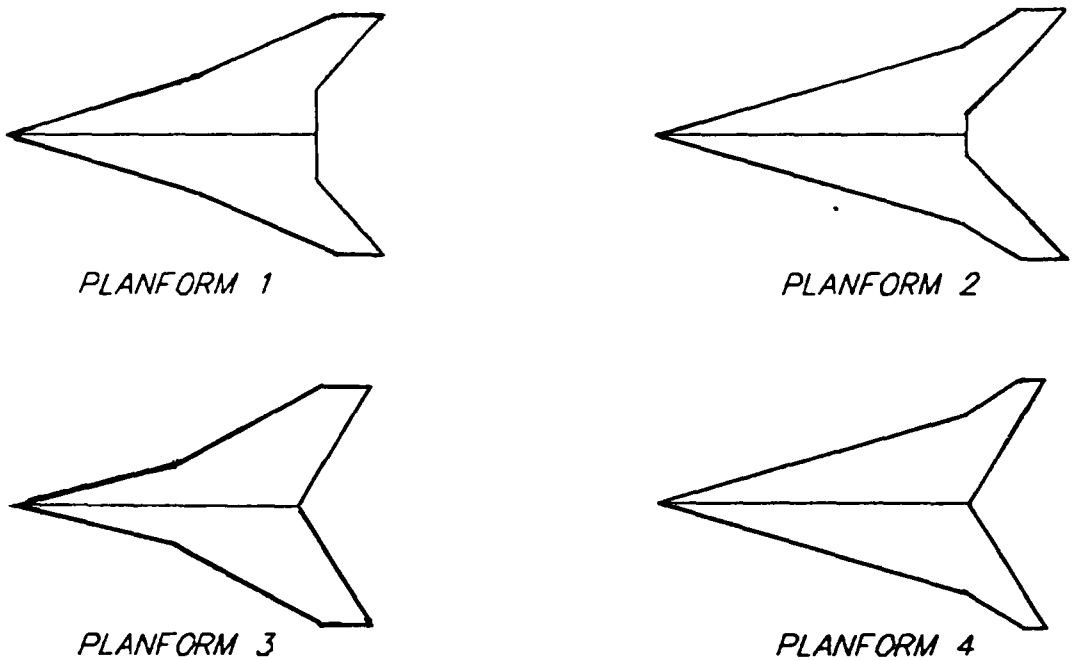

Figure 1.- Wing planform geometries.

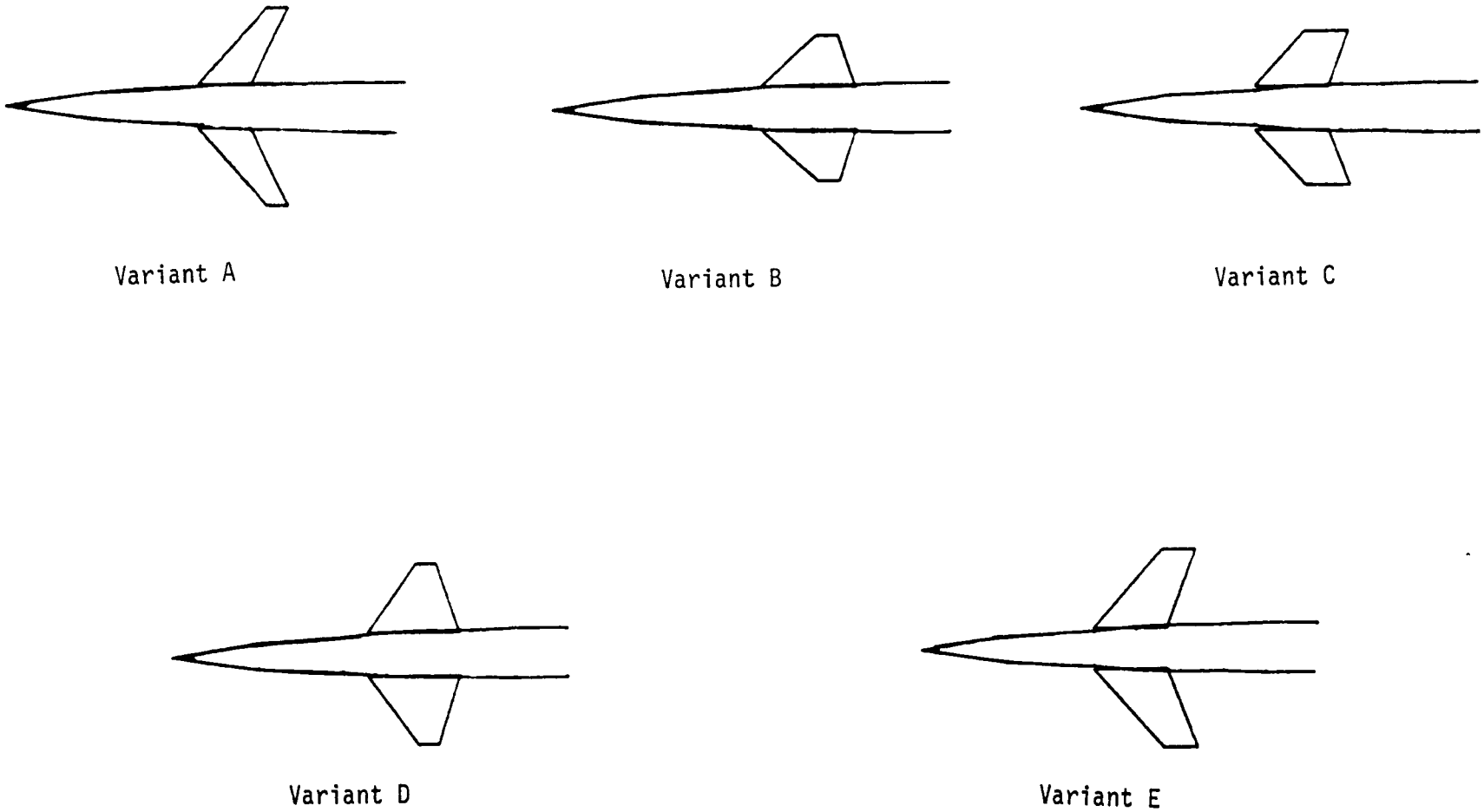

Figure 2.- Canard planform geometries.

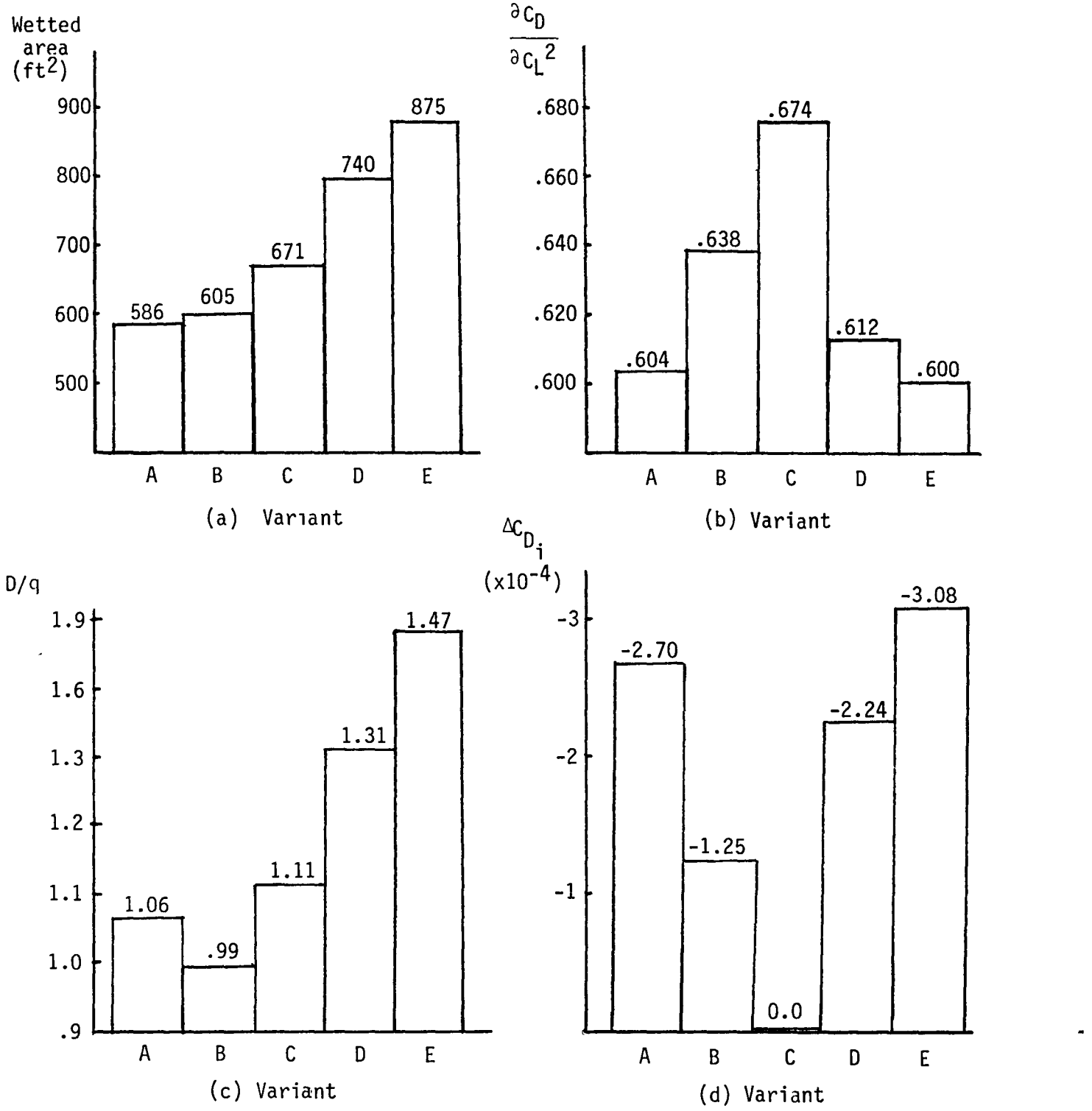

Figure 3.- Canard performance characteristics.

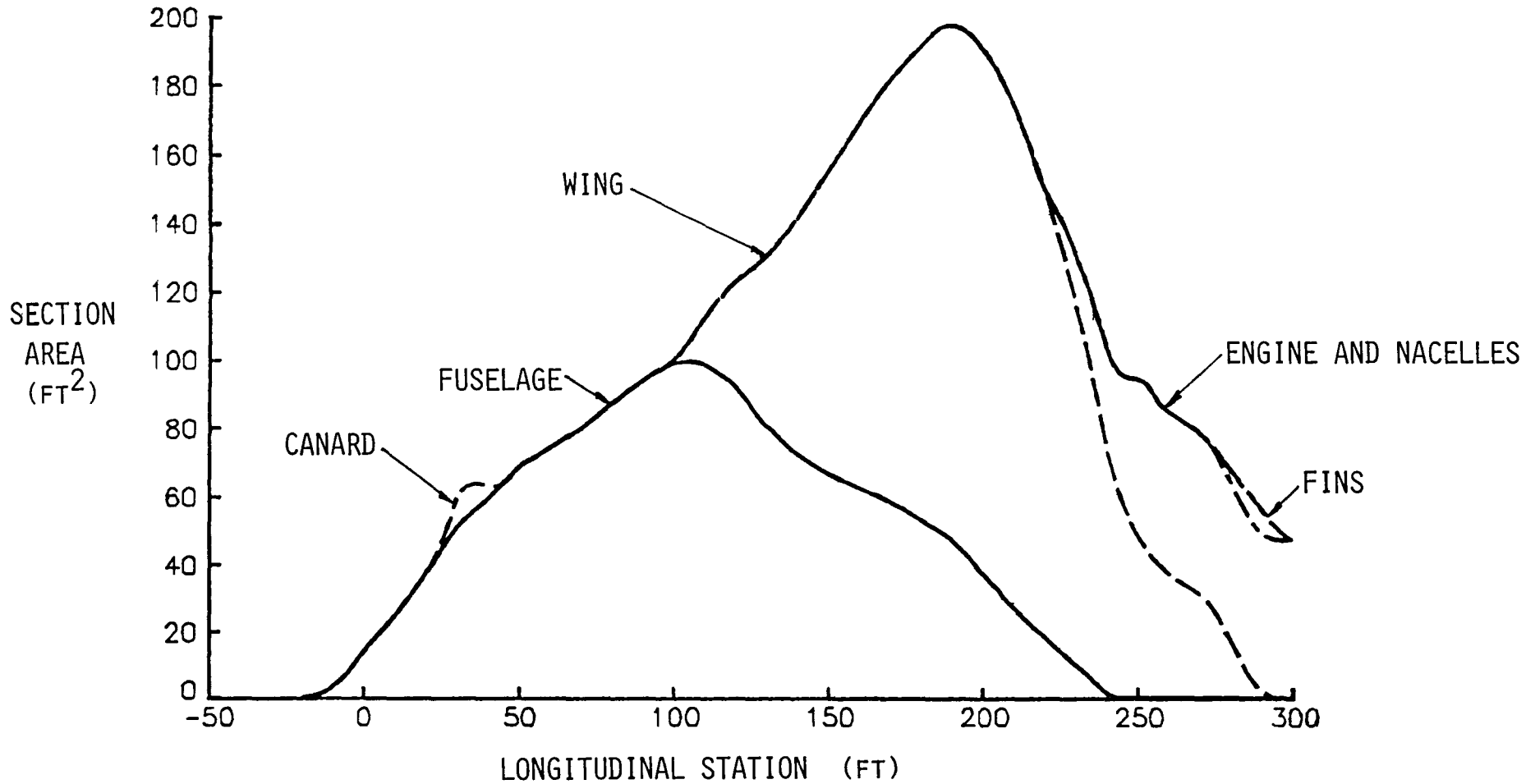

Figure 4.- Aircraft volume distribution.

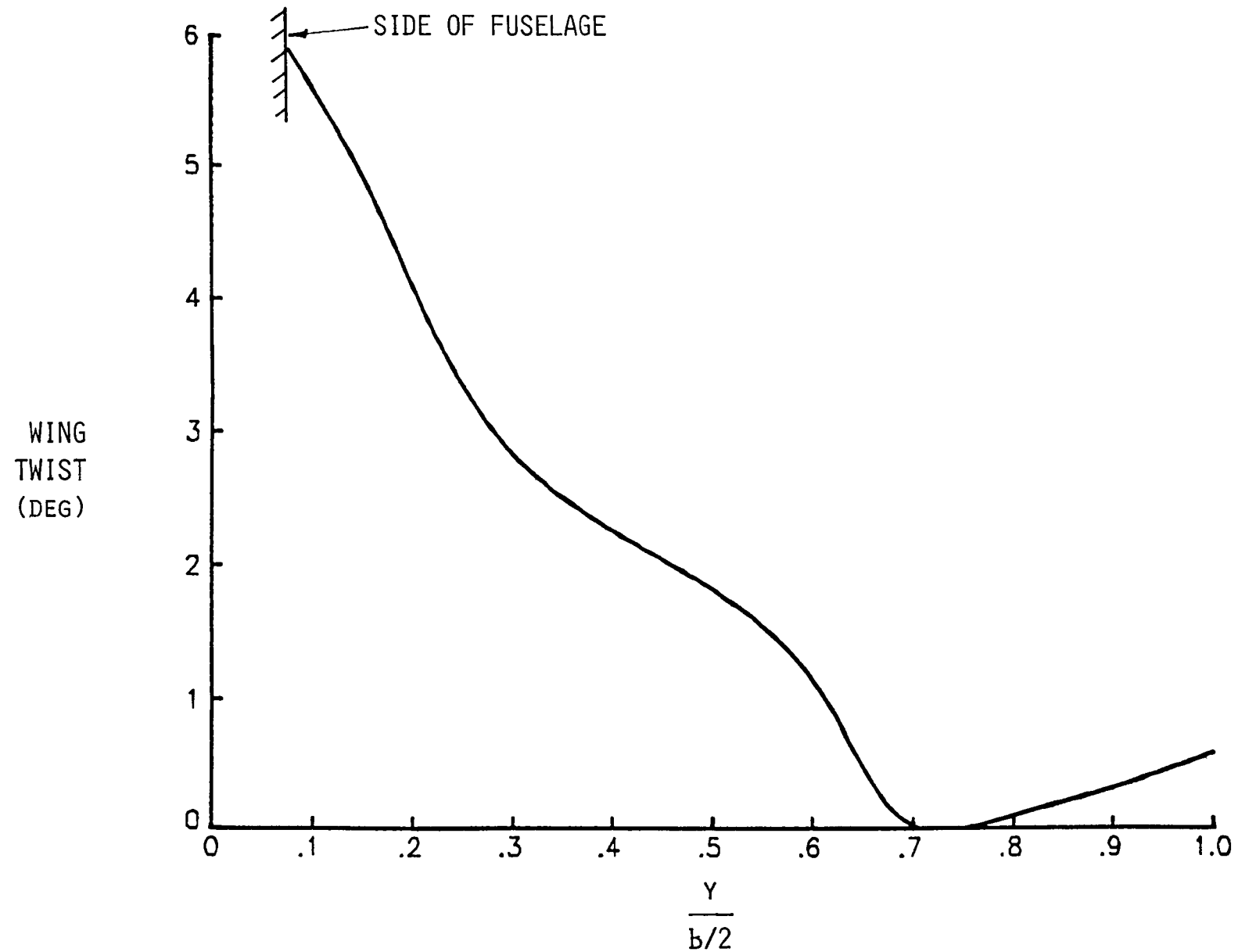

Figure 5.- Wing twist distribution.

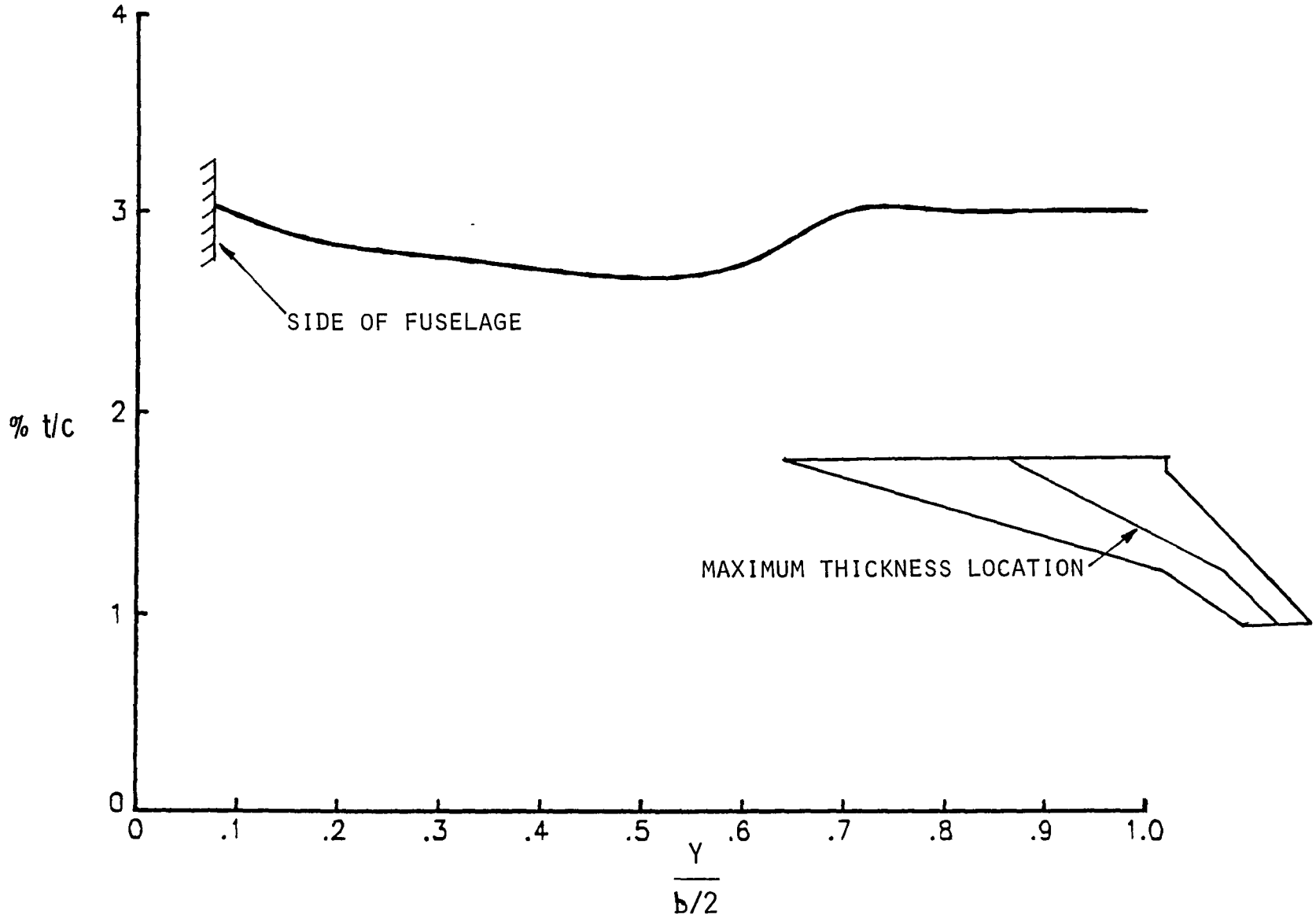

Figure 6.- Wing thickness distribution.

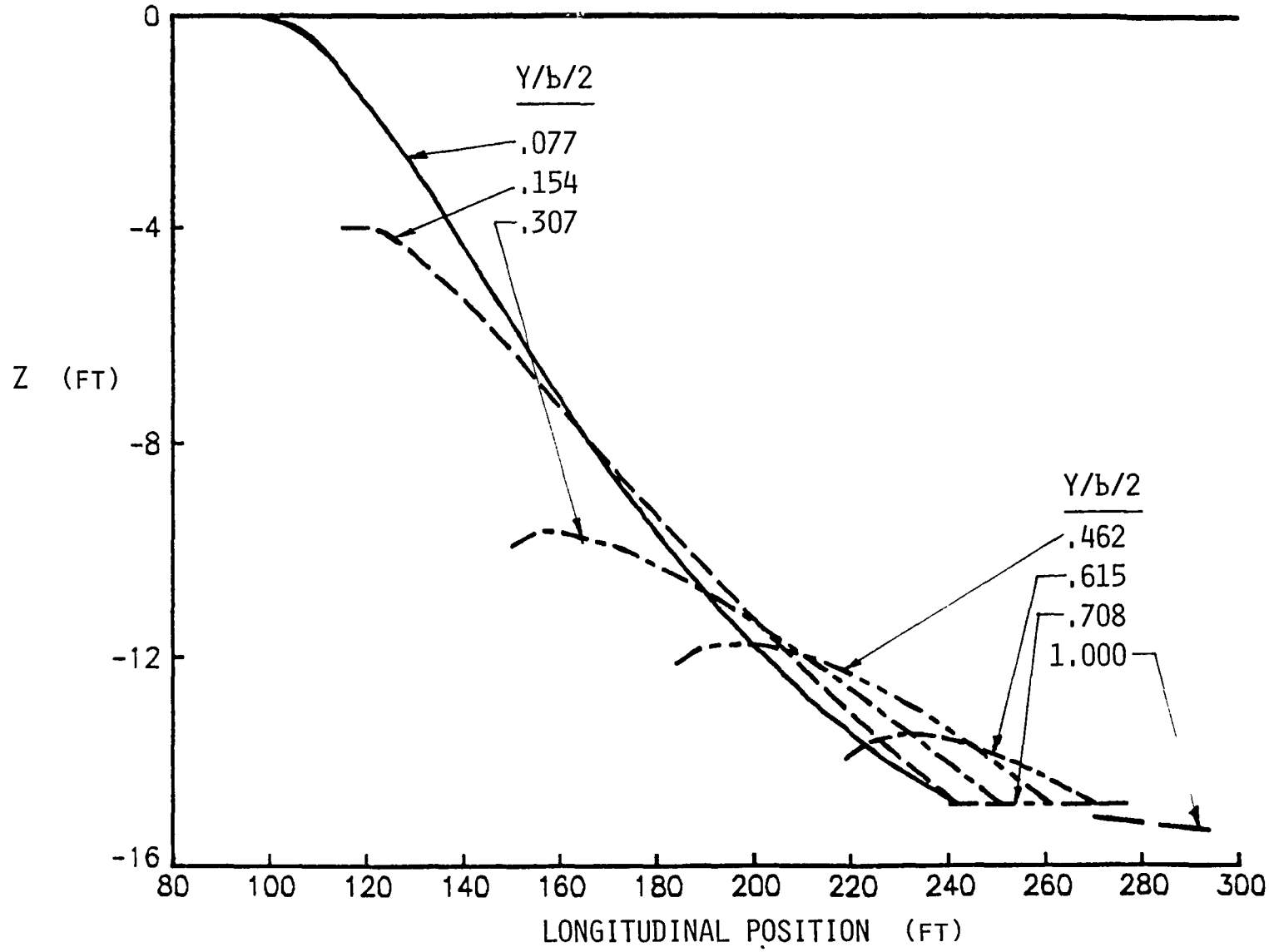

Figure 7.- Wing camber distribution.

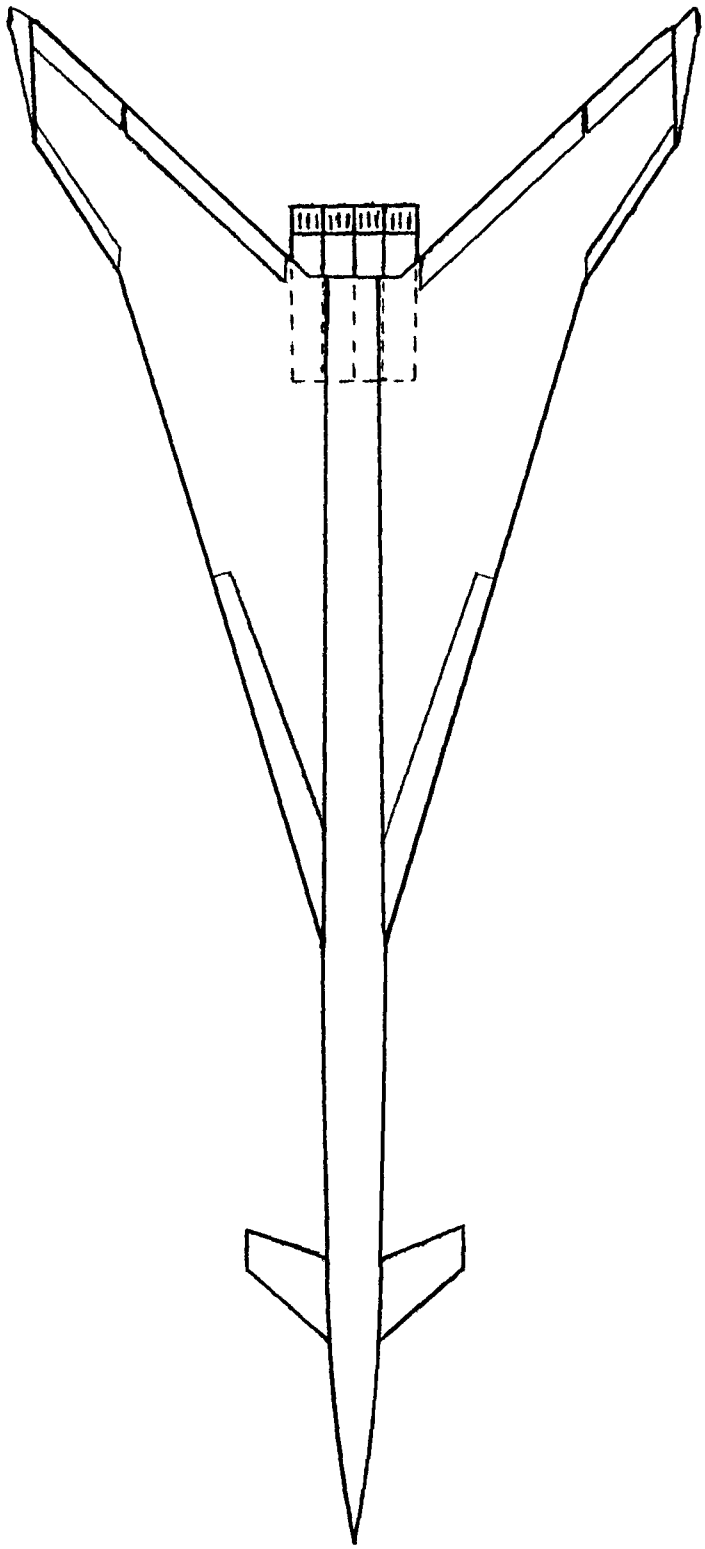

Figure 8a.- Top view of final configuration.

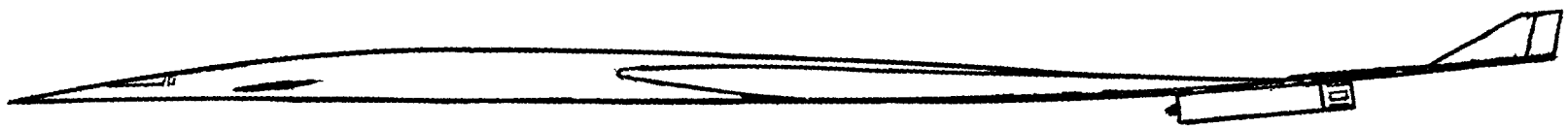

Figure 8b.- Side view of final configuration.

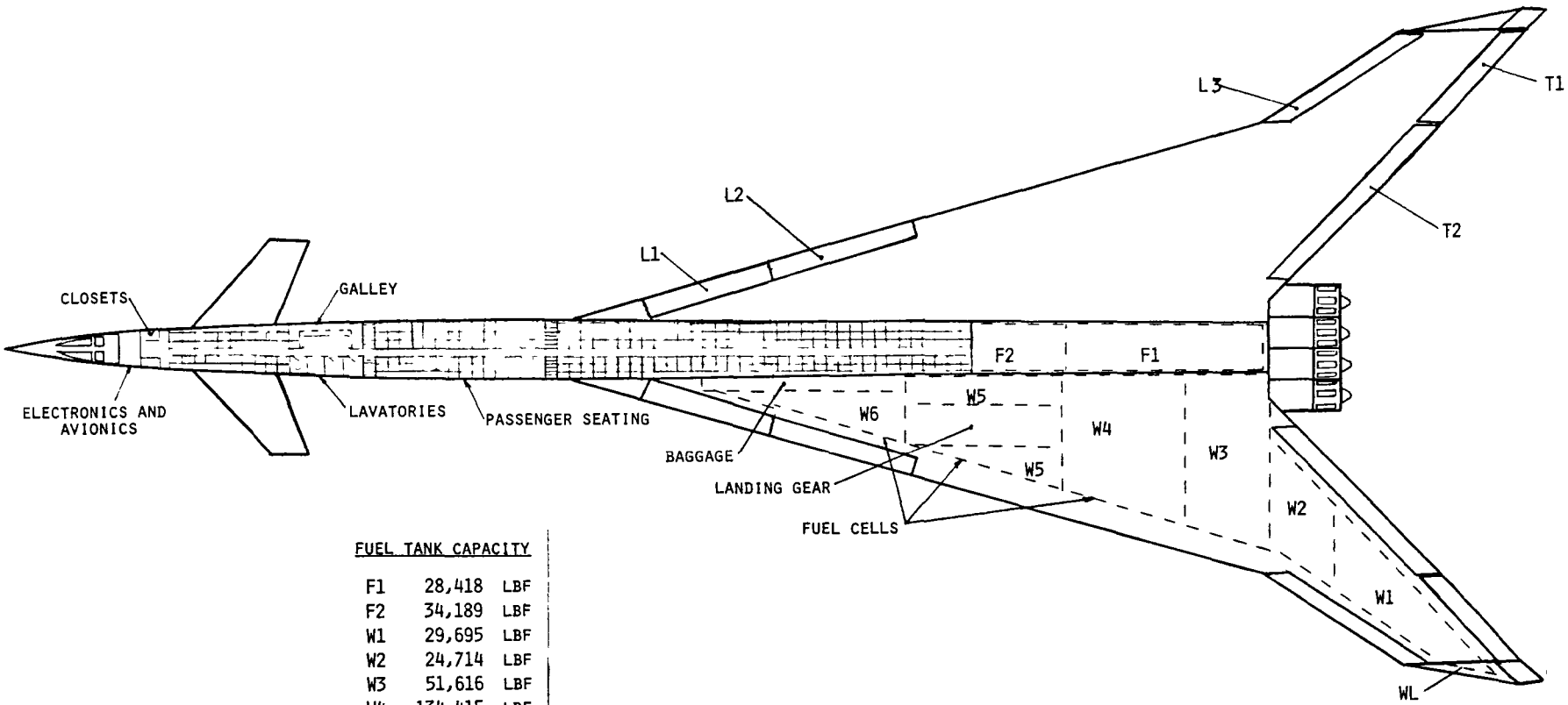

FUEL TANK CAPACITY		
F1	28,418	LBF
F2	34,189	LBF
W1	29,695	LBF
W2	24,714	LBF
W3	51,616	LBF
W4	134,415	LBF
W5	82,218	LBF
W6	23,631	LBF
WL	5,600	LBF

Figure 9.- Interior arrangement.

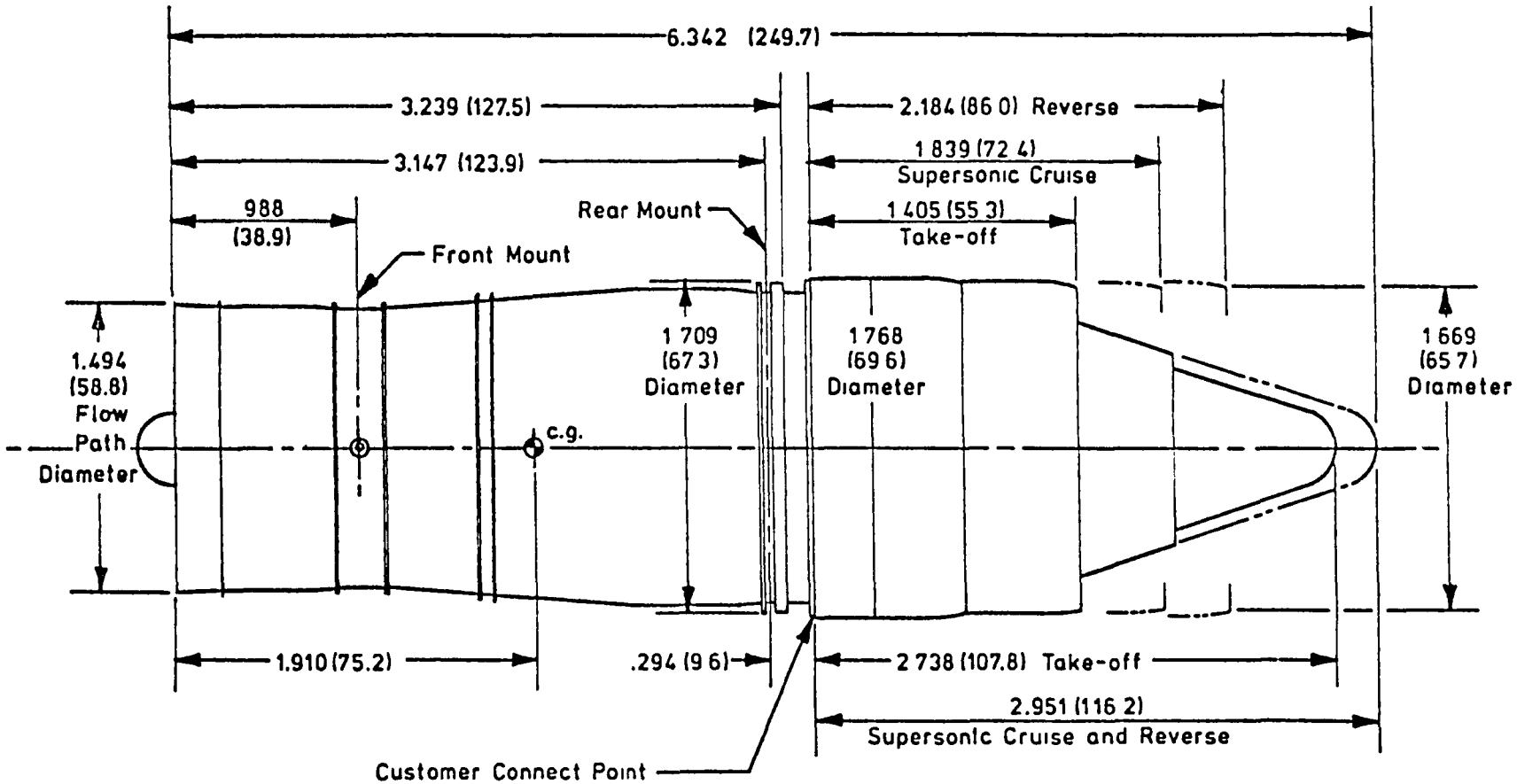

Figure 10.- GE21/J11-B14a engine.

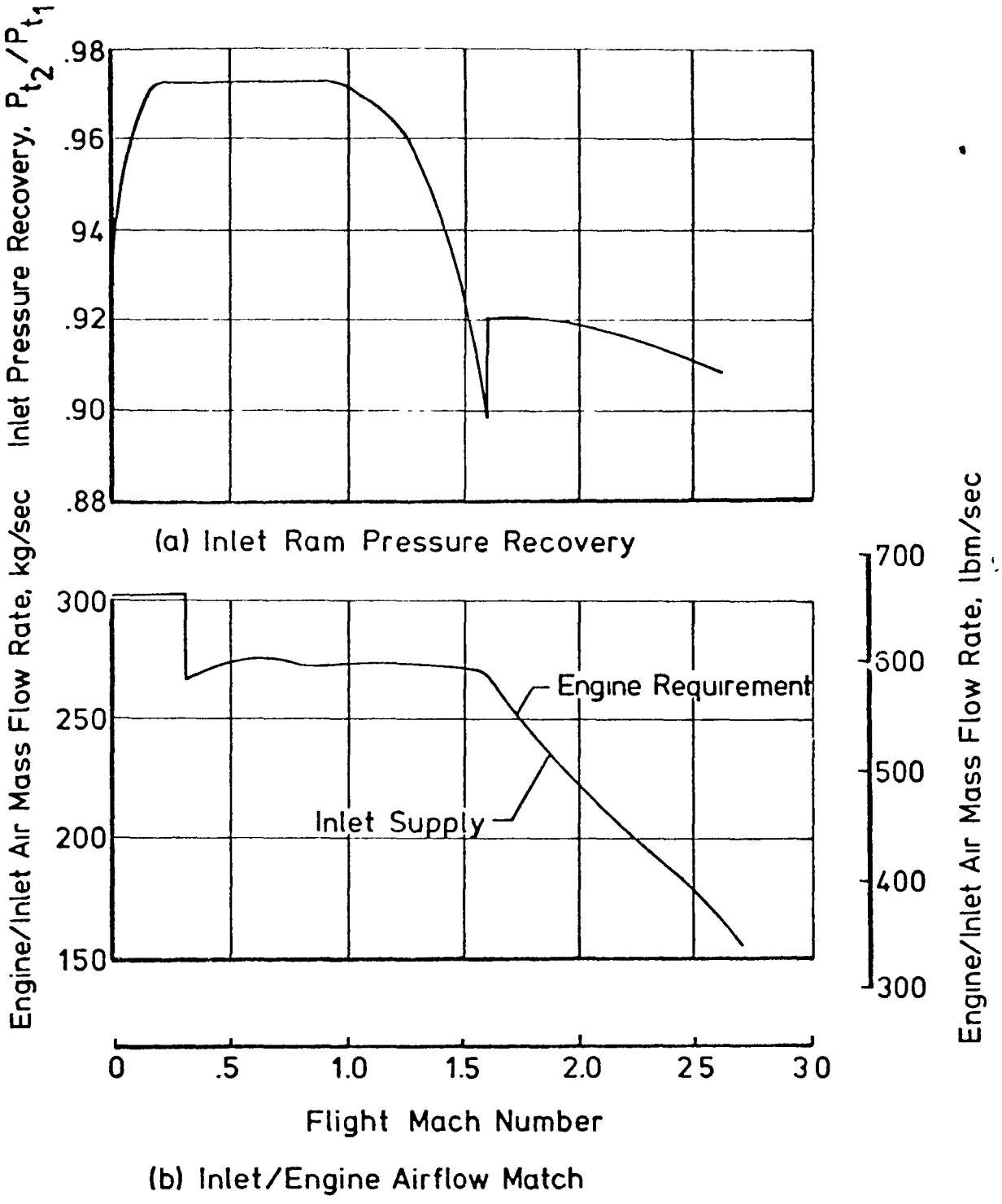

Figure 11.- NASA "P" inlet performance.

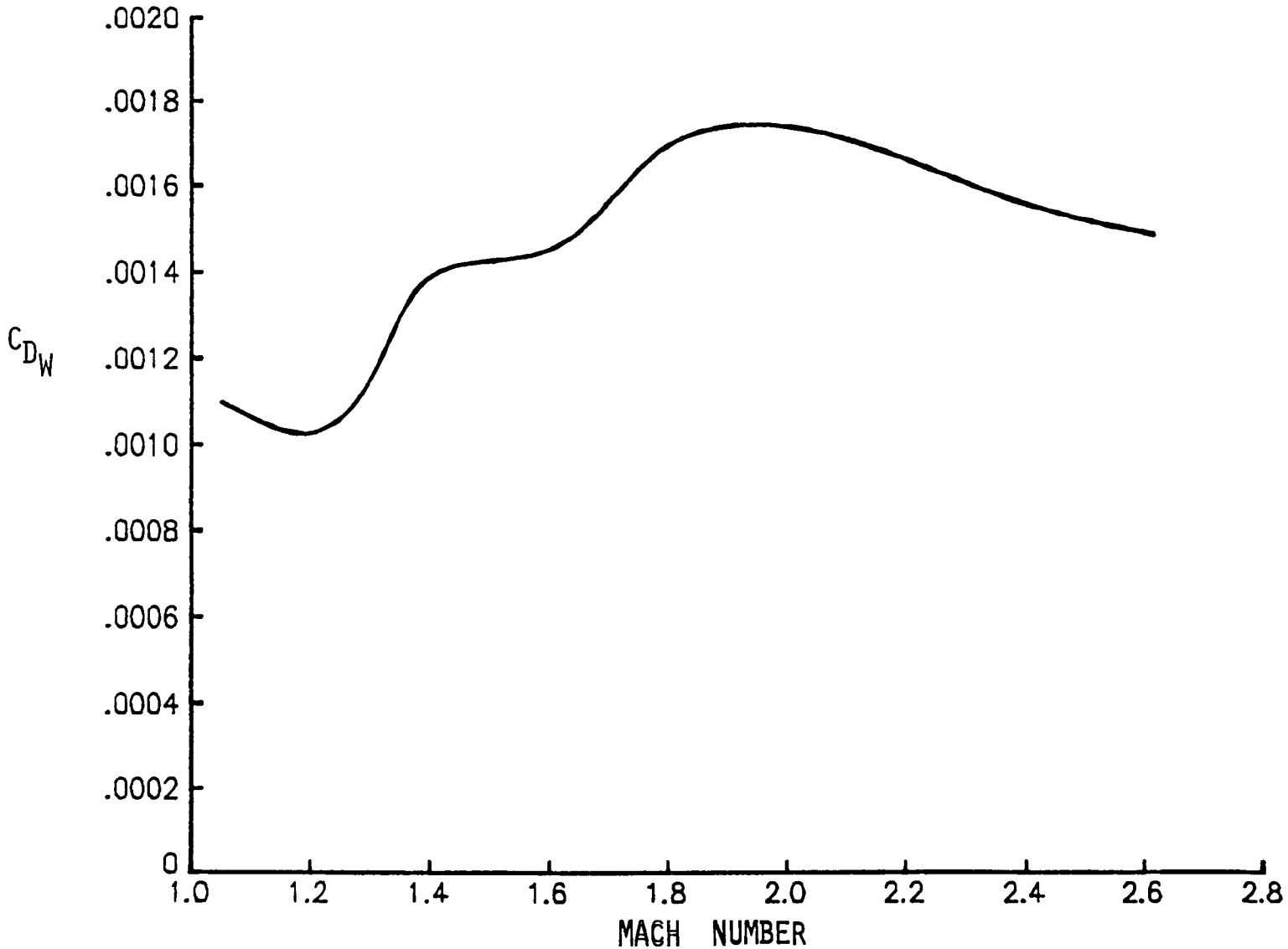

Figure 12.- Wave drag versus Mach number.

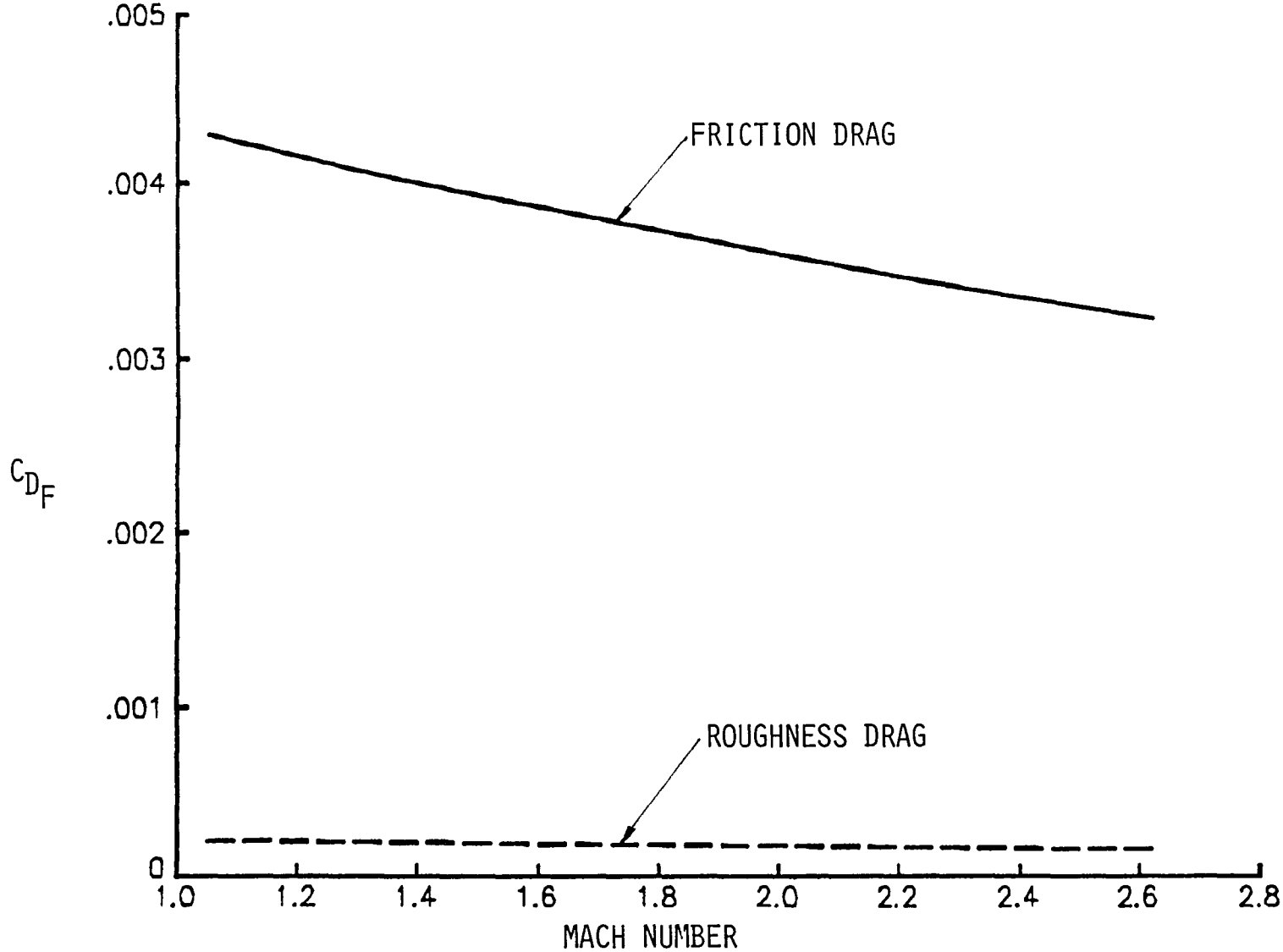

Figure 13.- Friction and roughness drag versus Mach number.

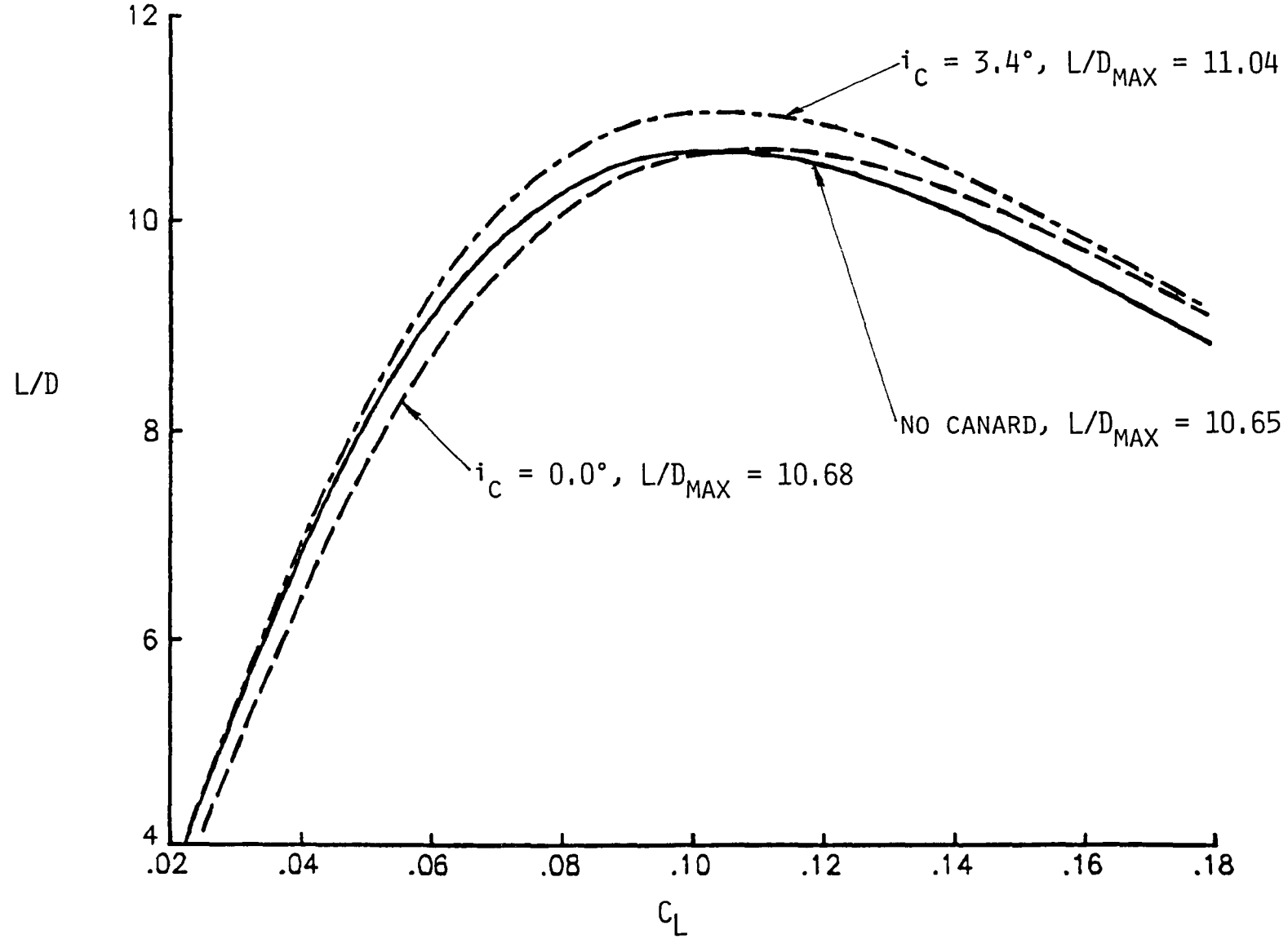

Figure 14.- Untrimmed L/D performance as a function of C_L and canard incidence, Mach 2.62, 55,000 feet.

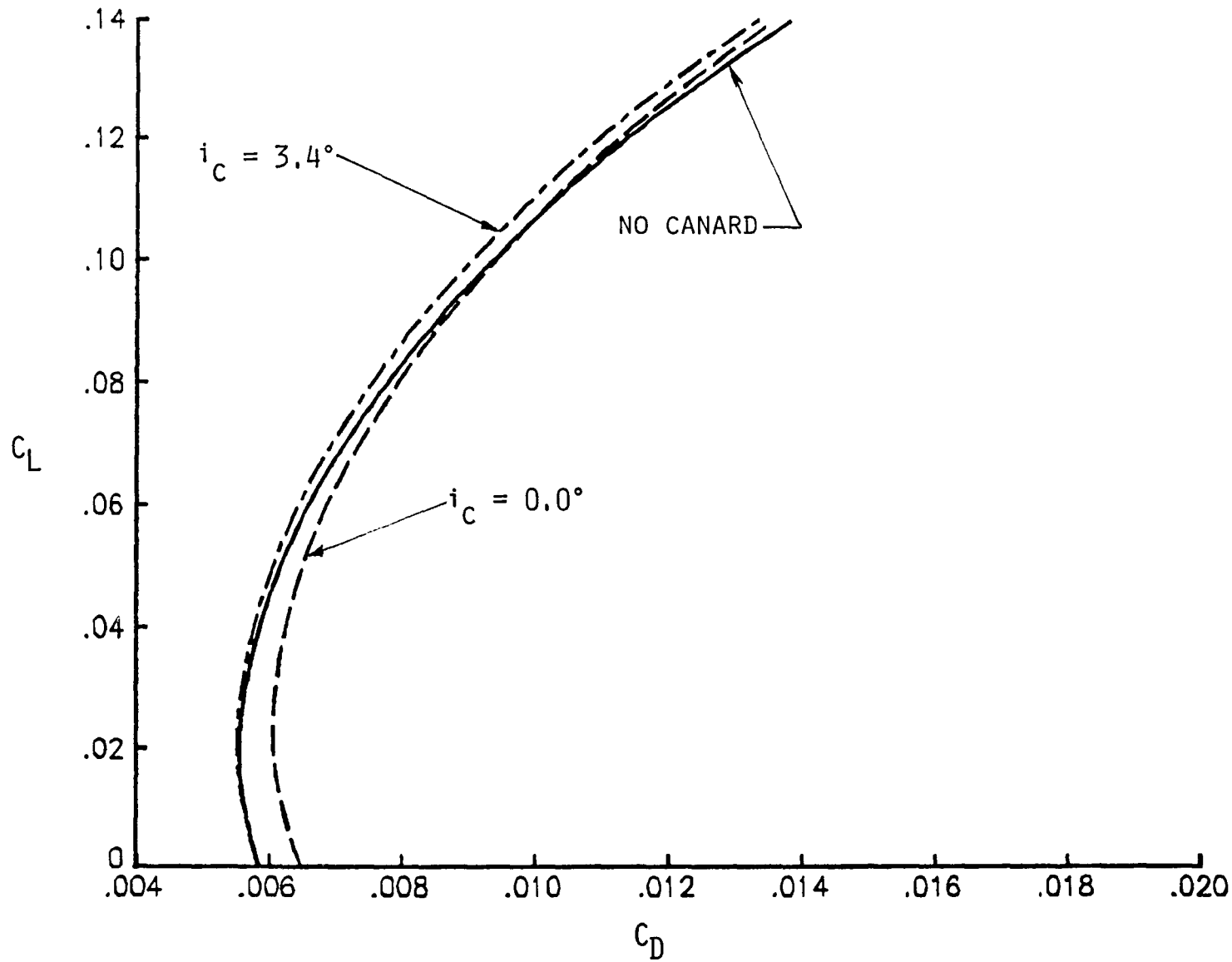

Figure 15.- Untrimmed drag polars as a function of canard incidence, Mach 2.62, 55,000 feet.

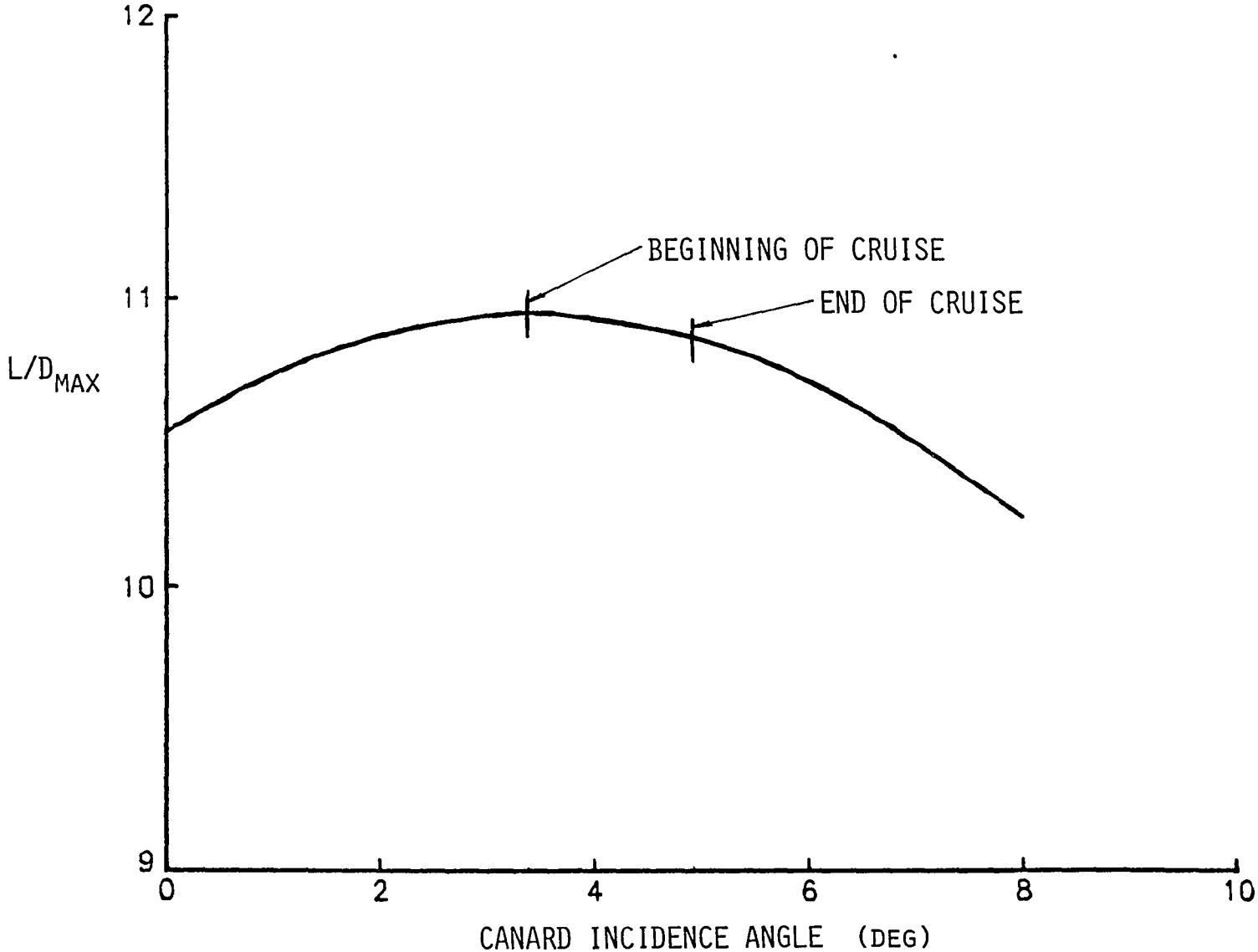

Figure 16.- Maximum lift-drag ratio as a function of canard incidence, Mach 2.62, 55,000 feet.

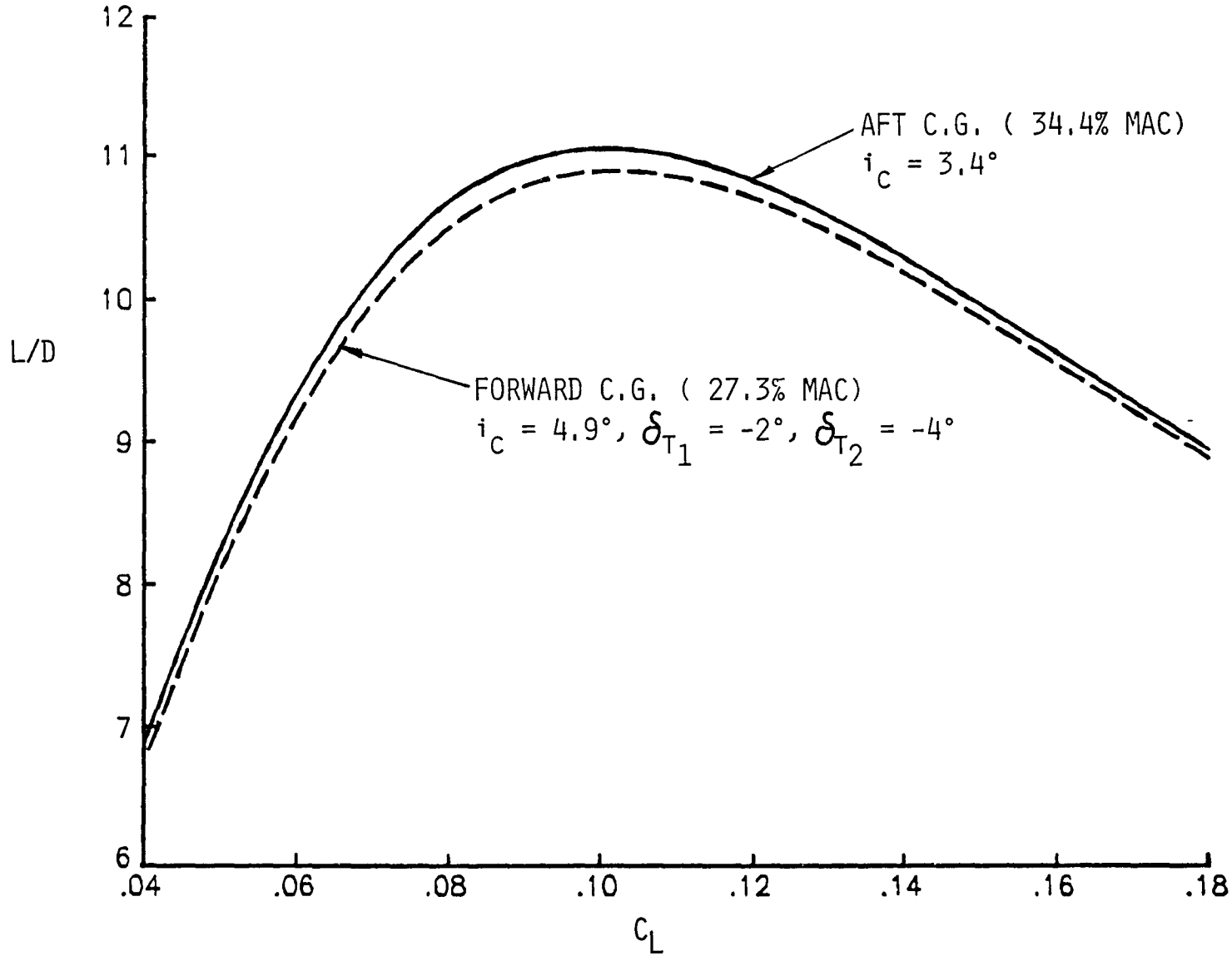

Figure 17.- Trimmed cruise L/D performance as a function of C_L, Mach 2.62, 55,000 feet.

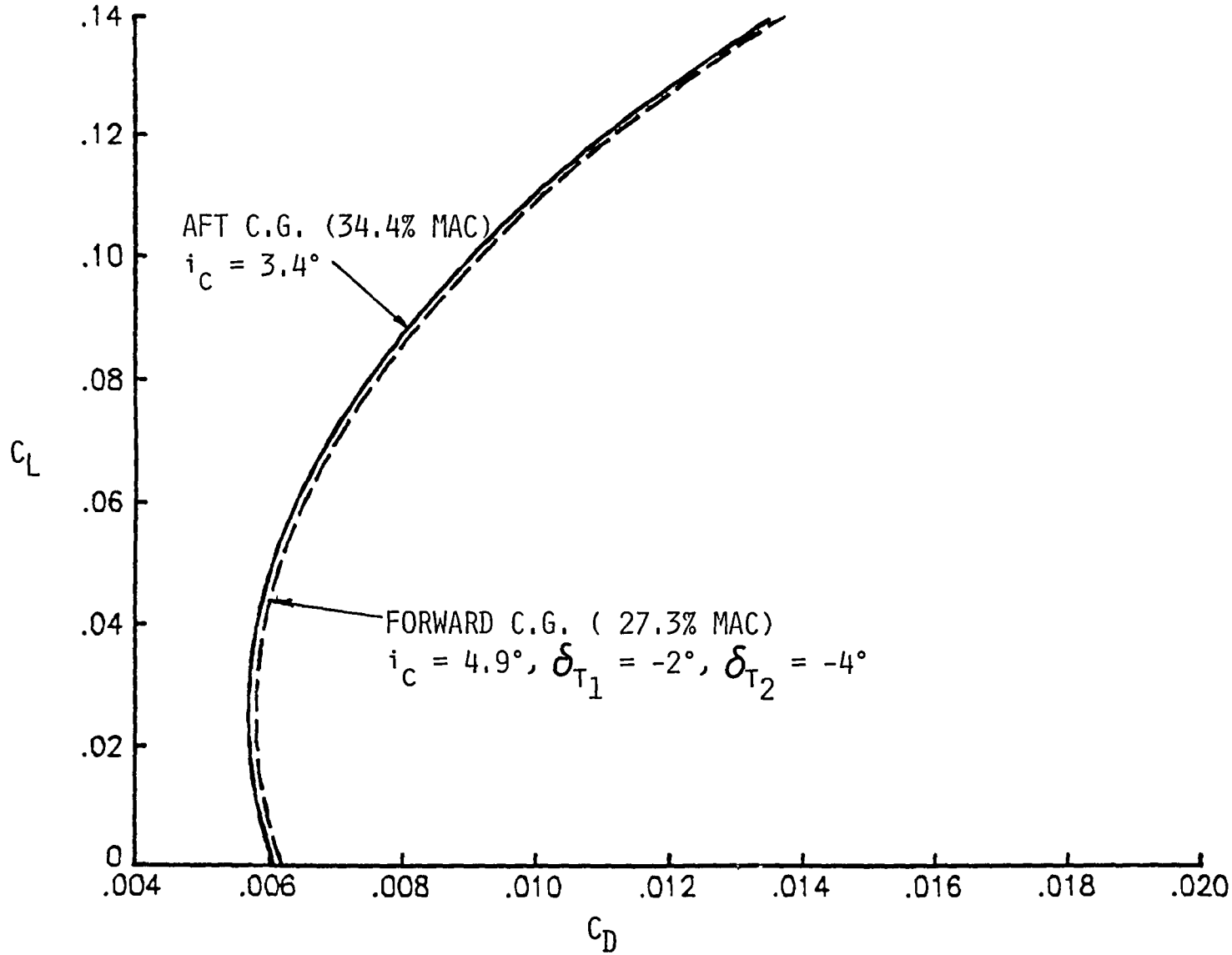

Figure 18.- Trimmed cruise drag polars, Mach 2.62, 55,000 feet.

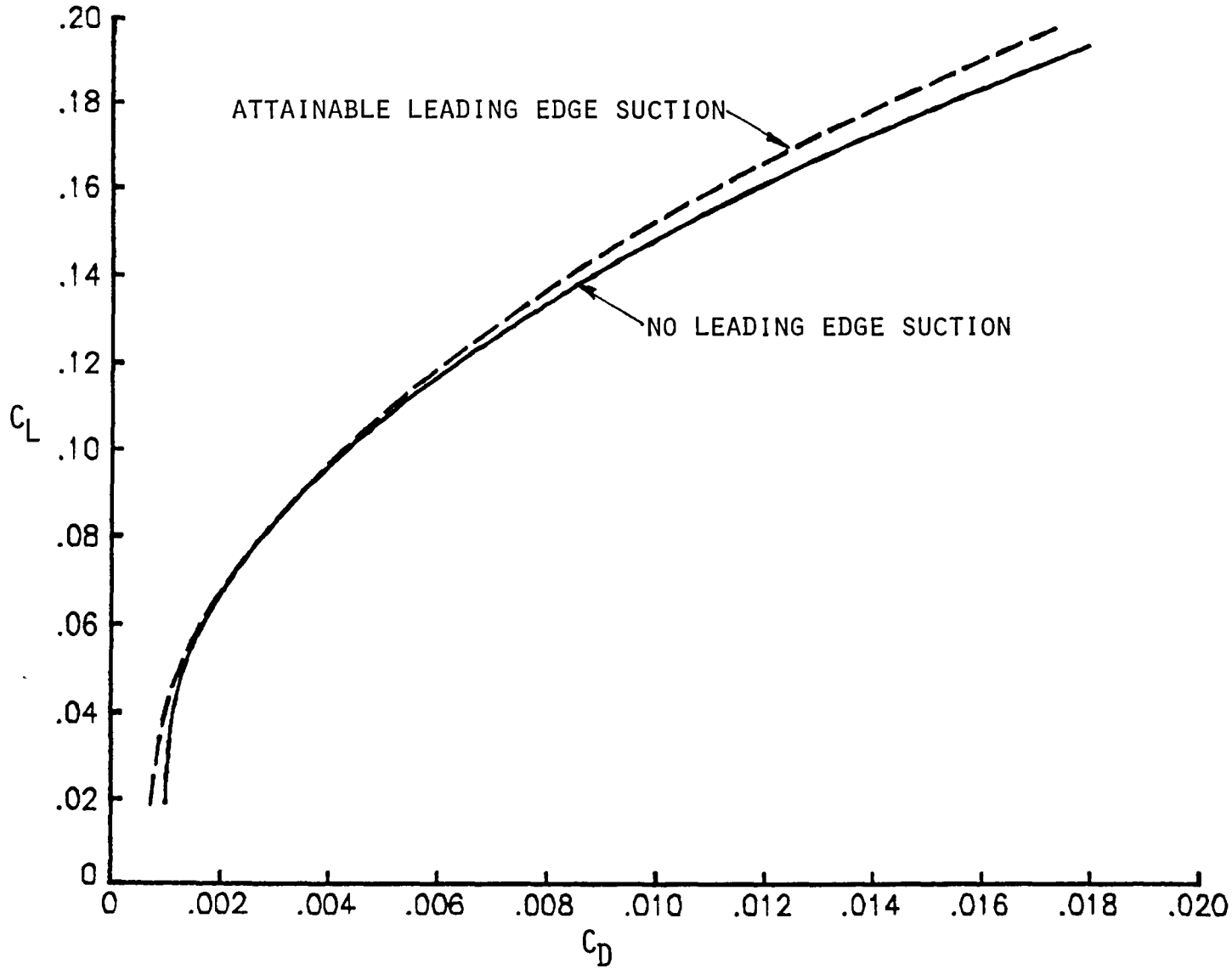

Figure 19.- Attainable leading-edge suction at cruise, Mach 2.62, 58,900 feet.

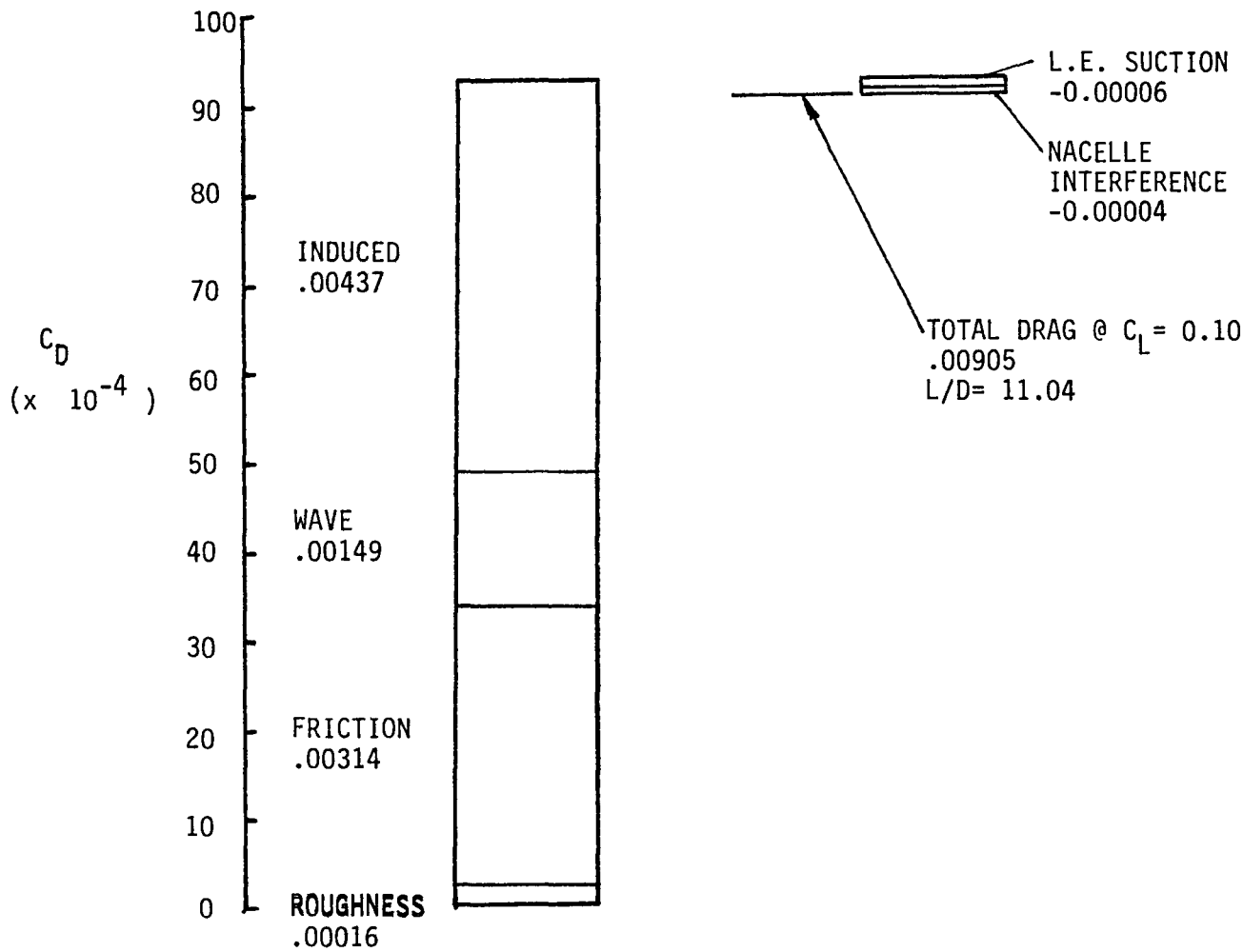

Figure 20.- Drag breakdown at maximum cruise L/D, C_L = 0.10, Mach 2.62, 55,000 feet.

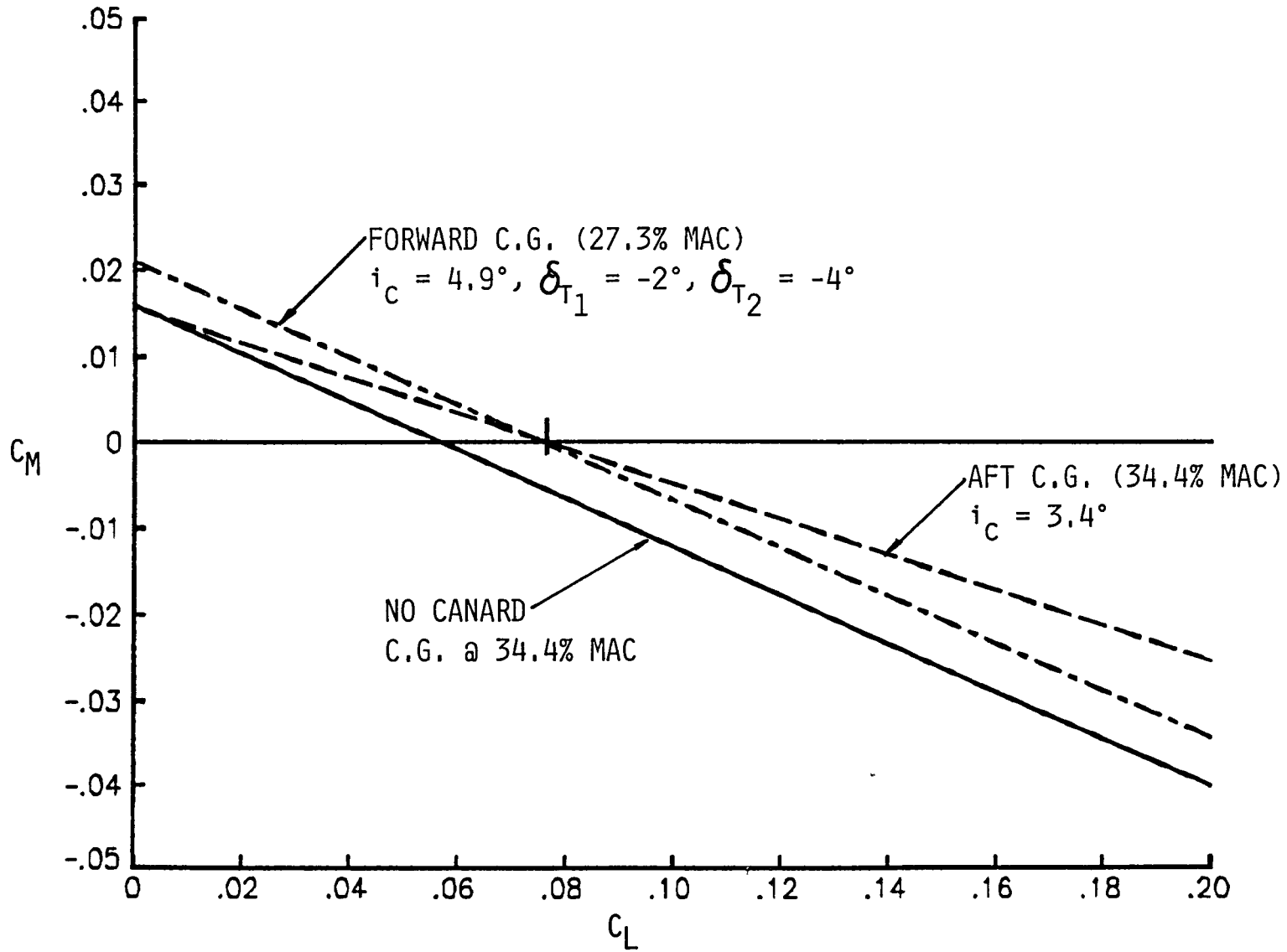

Figure 21.- Pitching moment as a function of C_L, c.g. location, and canard incidence, Mach 2.62, 55,000 feet.

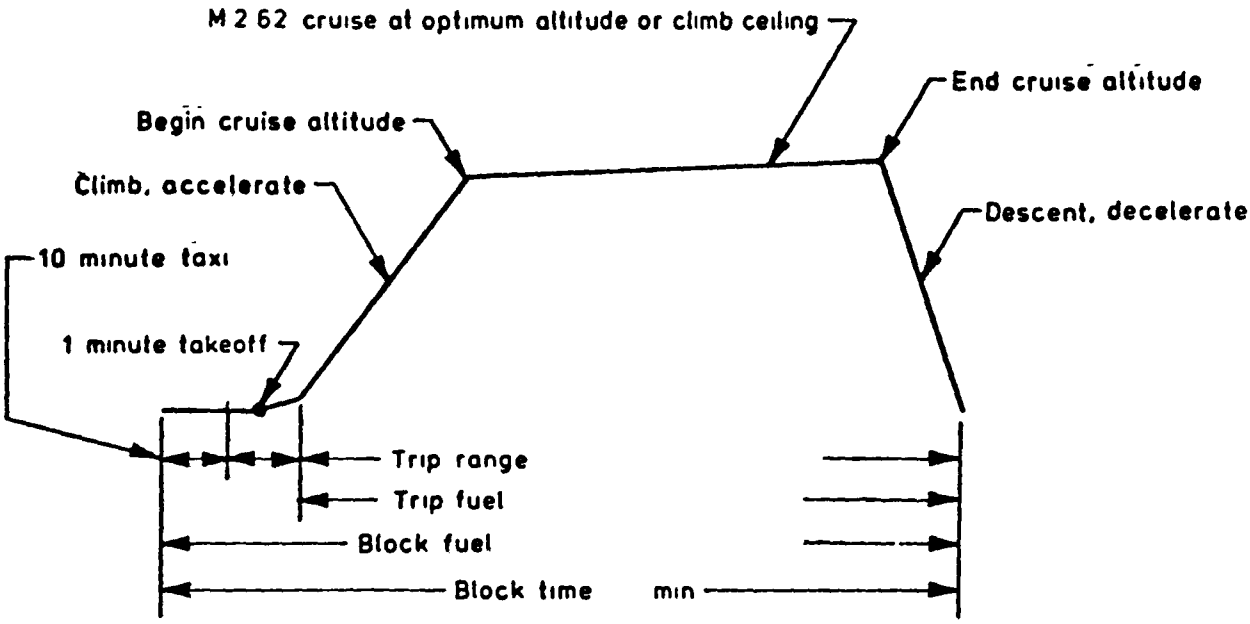

Note. CAB range = trip range minus traffic allowance as specified for supersonic aircraft.

(a) Primary Mission

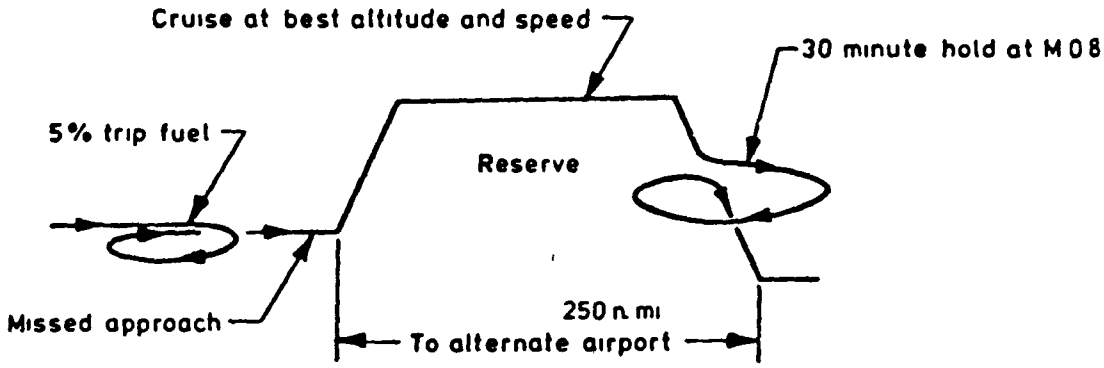

(b) Reserve Allowance Mission

Figure 22.- Mission profile.

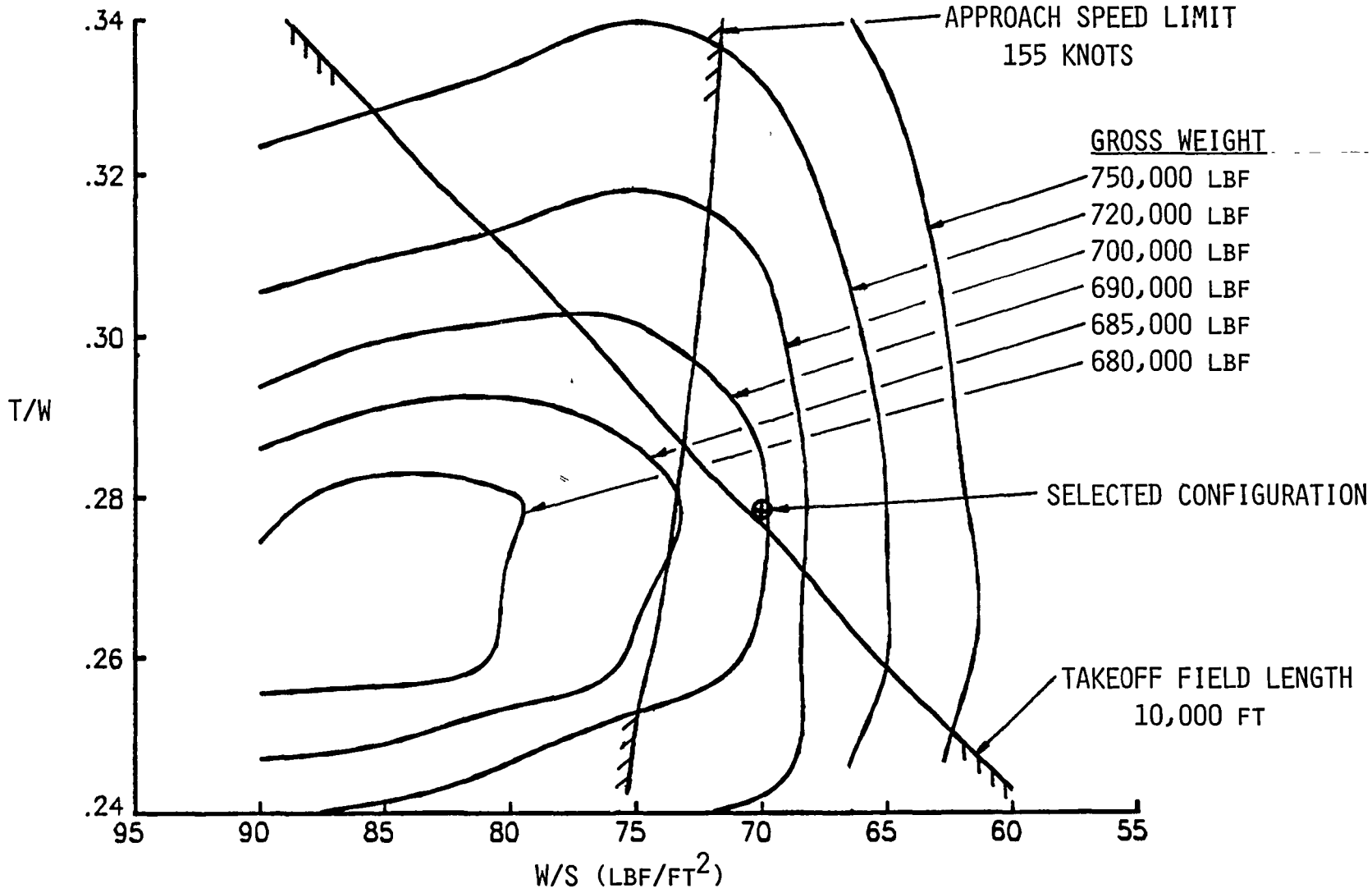

Figure 23.- Sizing thumbprint for 6,000 nautical miles design range.

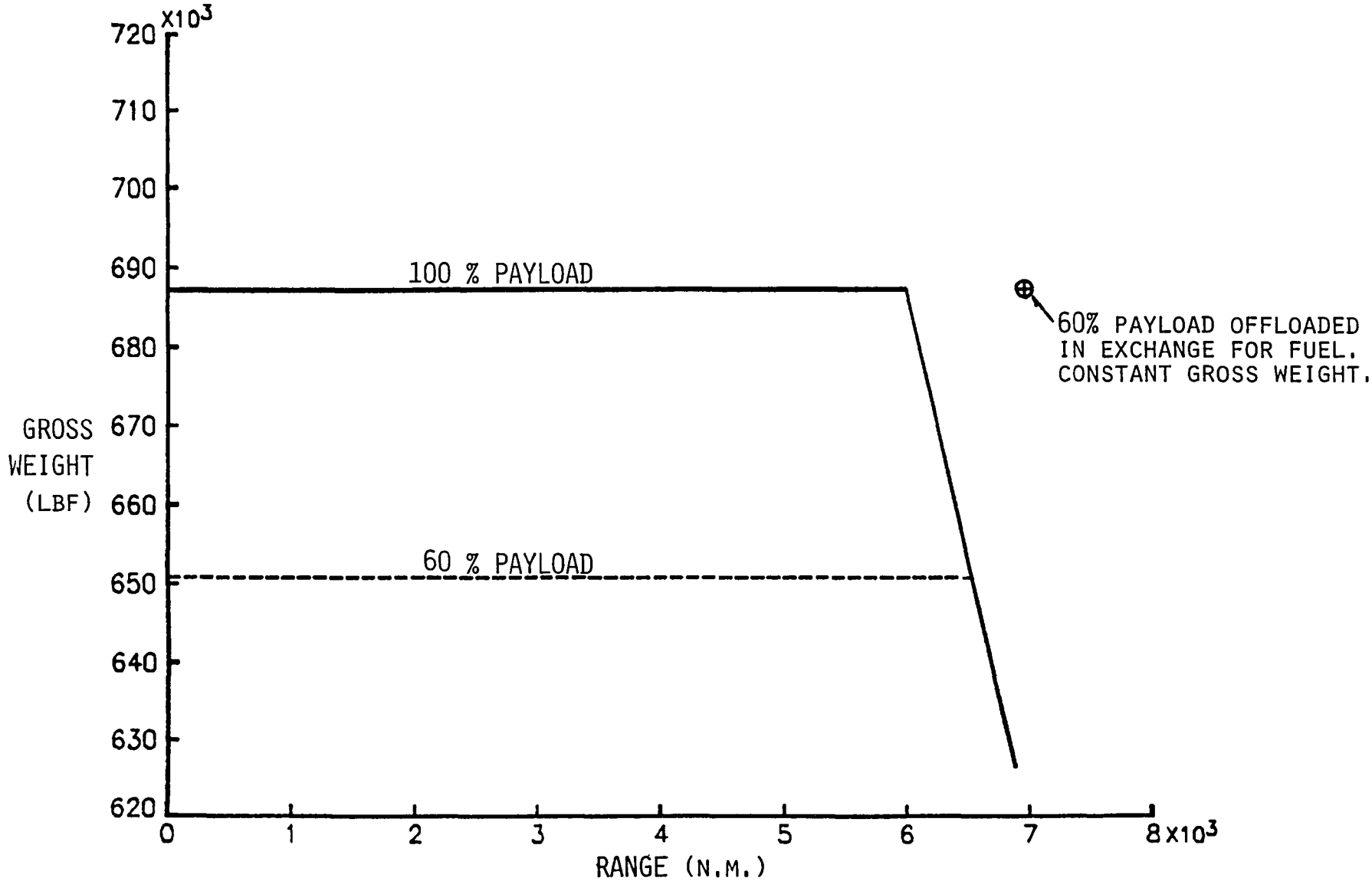

Figure 24.- Payload-range diagram.

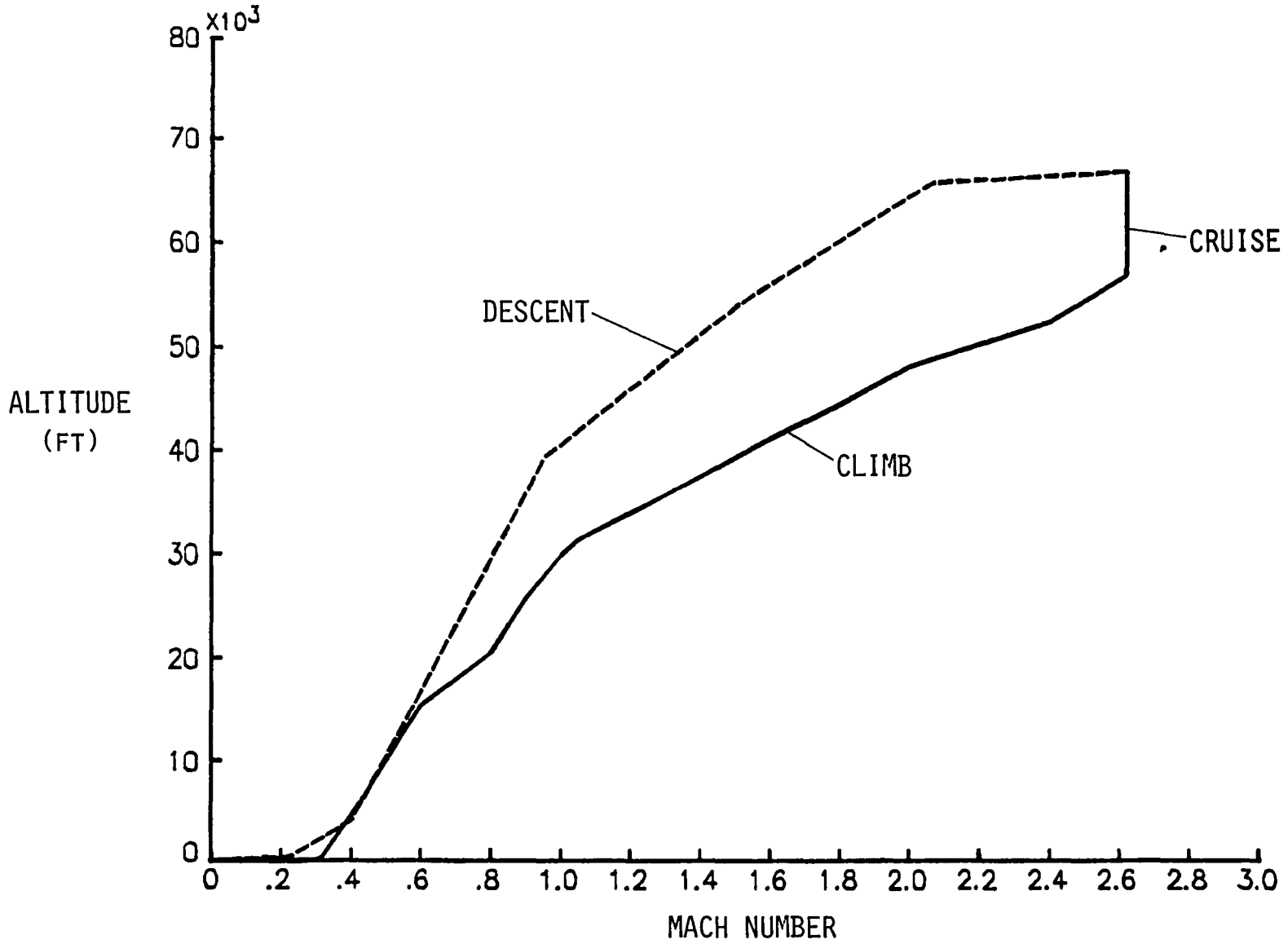

Figure 25.- Mach-altitude diagram.

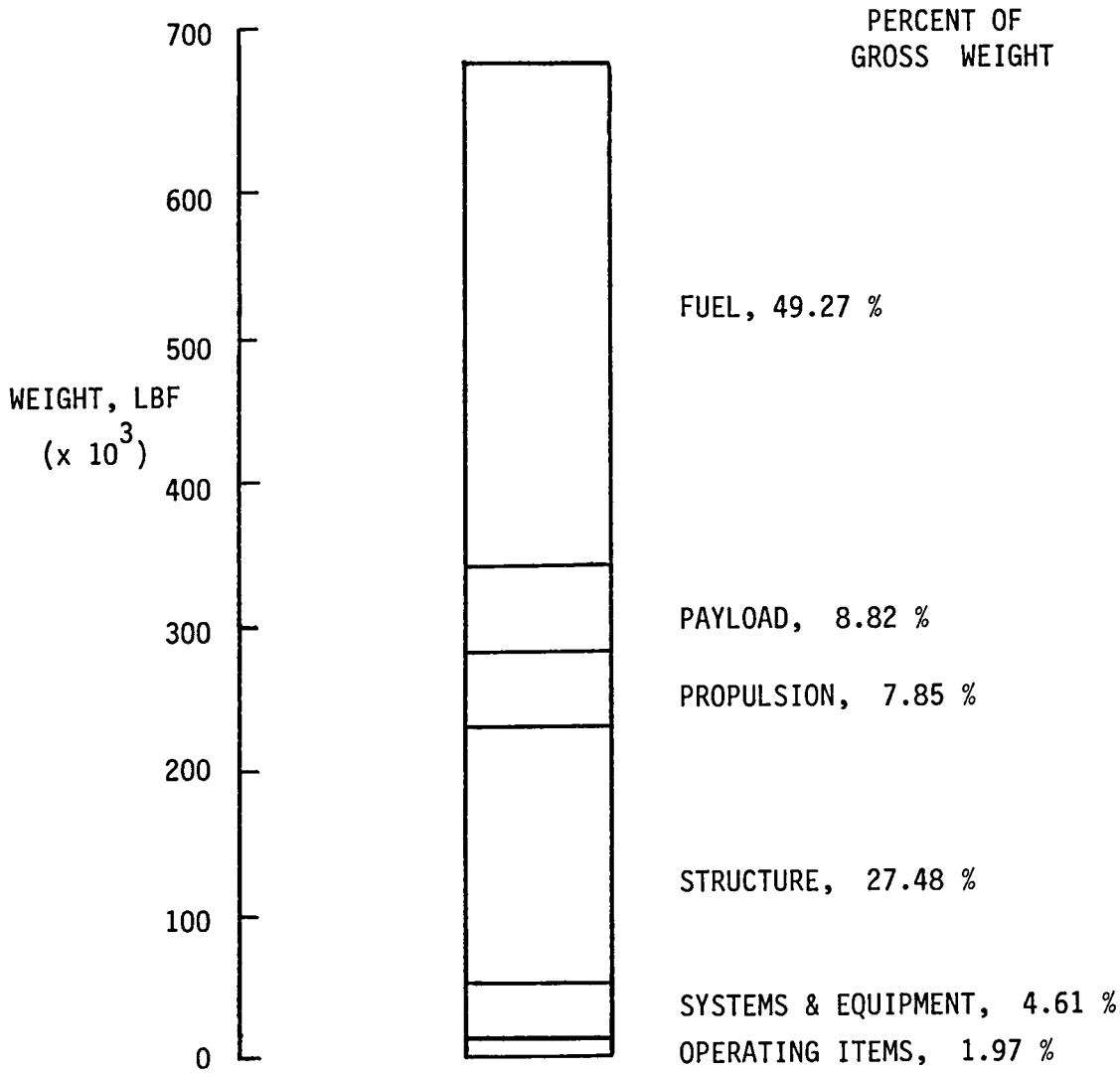

Figure 26.- Gross weight breakdown.

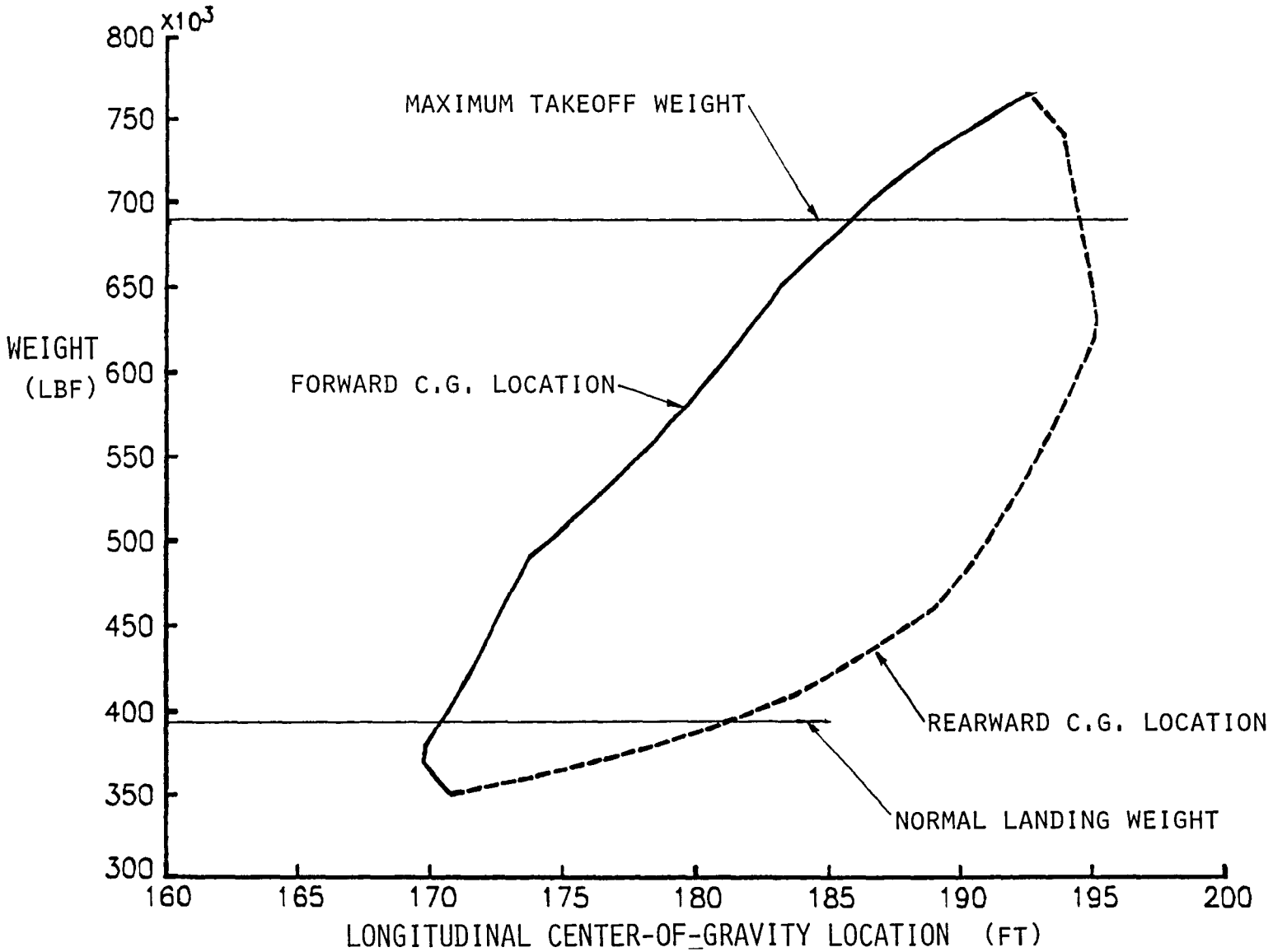

Figure 27.- Center-of-gravity envelope.

1 Report No	2 Government Accession No	3 Recipient's Catalog No
NASA TM-86414		

4 Title and Subtitle	5 Report Date
STUDY OF AN EFFICIENT LONG-RANGE MACH 2.7 SUPERSONIC TRANSPORT CONFIGURATION CONCEPT	July 1985
	6 Performing Organization Code: 505-43-43-01
7 Author(s): Peter D. Gall	8 Performing Organization Report No
	10 Work Unit No
9 Performing Organization Name and Address: NASA Langley Research Center, Hampton, VA 23665	11 Contract or Grant No
	13 Type of Report and Period Covered: Technical Memorandum
12 Sponsoring Agency Name and Address: National Aeronautics and Space Administration, Washington, DC 20546	14 Sponsoring Agency Code

15 Supplementary Notes

16 Abstract

A long-range Mach 2.7 supersonic transport configuration concept has been studied utilizing linear theory methods. The configuration was sized to carry 290 passengers 6,000 nautical miles nonstop. The final configuration has a maximum takeoff gross weight of 687,200 pounds, a wing loading of 69.8 lbf/ft^2, and a thrust-weight ratio of .278. The most significant result is that a significantly improved trimmed maximum lift-drag ratio of 11.04 can be obtained for a supersonic transport at Mach 2.62 and 55,000 feet.

17 Key Words (Suggested by Author(s))	18 Distribution Statement
Supersonic cruise Configuration analysis Cruise performance Lift-drag ratio	Unclassified - Unlimited Subject Category 05

19 Security Classif (of this report)	20 Security Classif (of this page)	21 No of Pages	22 Price
Unclassified	Unclassified	52	A04

N-305 For sale by the National Technical Information Service, Springfield, Virginia 22161

End of Document